ISN 8H-20
PNA BP805

JOURNAL OF GEOPHYSICAL RESEARCH, VOL. 90, NO. B5, PAGES 3589-3615, APRIL 10, 1985

SEISMIC POTENTIAL FOR LARGE AND GREAT INTERPLATE EARTHQUAKES ALONG THE CHILEAN AND SOUTHERN PERUVIAN MARGINS OF SOUTH AMERICA: A QUANTITATIVE REAPPRAISAL

Stuart P. Nishenko[1]

Lamont-Doherty Geological Observatory of Columbia University
Palisades, New York

Abstract. The seismic potential of the Chilean and southern Peruvian margins of South America is reevaluated to delineate those areas or segments of the margin that may be expected to experience large or great interplate earthquakes within the next 20 years (1984-2004). Long-term estimates of seismic potential (or the conditional probability of recurrence within a specified period of time) are based on (1) statistical analysis of historic repeat time data using Weibull distributions and (2) deterministic estimates of recurrence times based on the time-predictable model of earthquake recurrence. Both methods emphasize the periodic nature of large and great earthquake recurrence, and are compared with estimates of probability based on the assumption of Poisson-type behavior. The estimates of seismic potential presented in this study are long-term forecasts only, as the temporal resolution (or standard deviation) of both methods is taken to range from ±15% to ±25% of the average or estimated repeat time. At present, the Valparaiso region of central Chile (32°-35°S) has a high potential or probability of recurrence in the next 20 years. Coseismic uplift data associated with previous shocks in 1822 and 1906 suggest that this area may have already started to rerupture in 1971-1973. Average repeat times also suggest this area is due for a great shock within the next 20 years. Flanking segments of the Chilean margin, Coquimbo-Illapel (30°-32°S) and Talca-Concepcion (35°-38°S), presently have poorly constrained but possibly quite high potentials for a series of large or great shocks within the next 20 years. In contrast, the rupture zone of the great 1960 earthquake (37°-46°S) has the lowest potential along the margin and is not expected to rerupture in a great earthquake within the next 100 years. In the north, the seismic potentials of the Mollendo-Arica (17°-18°S) and Arica-Antofagasta (18°-24°S) segments (which last ruptured during great earthquakes in 1868 and 1877) are also high, but poorly constrained.

Introduction

The concept of seismic gaps provides the basic foundation for long-term earthquake forecasting [Fedotov, 1965; Mogi, 1968; Sykes, 1971; Kelleher, 1972; Kelleher et al., 1973; McCann et al., 1978, 1979; Nishenko and McCann, 1981]. Seismic gaps have been defined as those segments along active convergent or transform plate boundaries that have not experienced a repeat of a large or great interplate earthquake for more than a few decades and thus are considered likely sites for future large or great events. While these observations provide estimates as to the location and maximum likely size of future earthquakes, they do not provide estimates to better than a few tens of years as to the time of occurrence of future large shocks. The lack of more precise temporal estimates primarily reflects the absence of local recurrence time, source size and plate velocity data in the definition of the categories of seismic potential.

McCann et al. [1978, 1979] and Nishenko and McCann [1981] have qualitatively used the term seismic potential to mean the likelihood of a region to have a large or great earthquake on a plate boundary within a specified period of time. Hence, a region of high seismic potential is a seismic gap, which for historic or tectonic reasons is considered likely to produce a large shock within the next few decades. The three major temporal categories used by McCann et al. [1978, 1979] and Nishenko and McCann [1981] to assess seismic potential are based on the shortest repeat times observed (about 30 years) and an arbitrary cutoff of 100 years (category 1: $t>100$ years; category 2: $30<t<100$ years; category 6: $t<30$ years; where t is the time elapsed since the last large or great earthquake). Experience with the map of seismic potential by McCann et al. [1978, 1979] and Nishenko and McCann [1981] has shown that most large shocks since 1978 have occurred in areas designated categories 2 and 3 (category 3: areas where the historic record is incomplete). No shocks have occurred in those segments designated category 1, the highest potential. This is not too surprising, as many of those regions assigned to category 1 by McCann et al. [1978, 1979] produce very great shocks ($M_w=9$) with long repeat times, and are few in number compared to those regions in category 2. This discrepancy, however, suggests that the definition and assignment of areas to category 1, the zone of highest potential, should be revised to include recurrence time data and to reflect the imminence of an expected large shock probabilistically, rather than just by the amount of time elapsed.

This study applies both statistical and deterministic methods to assess the seismic potential or probability of recurrence along the Chilean and southern Peruvian margins and to denote those areas likely to produce large or great interplate earthquakes during the next 20 years (1984-2004). This time span is chosen to enable the evaluation of the forecasts and hence evaluation of the

[1]Now at U.S. Geological Survey, Denver, Colorado.

Copyright 1985 by the American Geophysical Union.

Paper number 4B0511.
0148-0227/85/004B-0511$05.00

models used to create these forecasts at a reasonable time in the future. The estimates presented in this study are long-term forecasts only, as the degree of temporal resolution (or standard deviation) of these techniques is estimated to be ±15% to ±25% of the repeat time. An advantage of quantifying the seismic gap concept is the capability of finer gradations or differentiations of seismic potential than was available with the more qualitative seismic gap designations. In addition, quantitative long-term forecasts enable disaster mitigation programs to be developed and focused on specific areas judged to have high levels of seismic hazard or potential.

Methods of Analysis

In this study, three techniques are used to provide quantitative estimates of seismic potential (i.e., the imminence of a large or great shock). The first method is based on a statistical description of historic repeat times using Weibull distribution analysis. This approach treats earthquake occurrence as the result of a stochastic process. The probabilities of recurrence are based solely on the frequency distribution of prior earthquake repeat times. The Weibull distribution is a useful description of failure time distributions, as it allows for a power law dependence of hazard rate as a function of time. Weibull distributions are widely used in quality control research and failure time statistics, where the failure times of industrial components do not fit simple normal or Gaussian distributions [Weibull, 1951; Mann et al., 1974; Kapur and Lamberson, 1977; Kalbfleisch and Prentice, 1980]. Recently, Rikitake [1975, 1976a,b] and Hagiwara [1974] applied Weibull statistics to crustal strain and earthquake repeat time data to determine the "failure time" and "strength" of the earth's crust for various seismogenic regions. The property of a time-dependent hazard rate is especially appealing to the seismic gap model, which suggests that the potential for a future great earthquake is small immediately following a great shock and grows with increasing time since the previous event. Brillinger [1982] and Sykes and Nishenko [1984] used Weibull distributions to describe repeat time behavior along the Pallett Creek and Parkfield-Cholame segments of the San Andreas fault in California.

The data set of large and great earthquake repeat times used for the Weibull analysis comes from catalogs of historic South American shocks compiled by Lomnitz [1970], Kelleher [1972] and Silgado [1973]. Historic descriptions of great shocks along the Peruvian and Chilean margins extend to the sixteenth century and cover three to four recurrence cycles in many areas. Variations in population density with time, however, have resulted in a historic catalog which is fairly complete in some areas and less complete in others. Hence, the accuracy of the forecasts varies spatially with the completeness of the catalogs. With the exception of shocks in zone 1 (Punta Arenas-Tierra del Fuego), all of the large and great shocks considered in this study are of the underthrust type and account for the majority of convergent motion between the Nazca and South

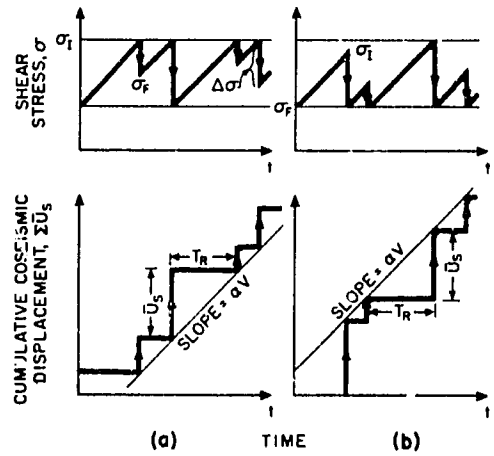

Fig. 1. Schematic slip histories for the time- and slip-predictable models of earthquake recurrence [after Bufe et al., 1977; Shimizaki and Nakata, 1980; and Sykes and Quittmeyer, 1981]. (a) Time-predictable model. Repeat time is proportional to the size (or amount of displacement) in the preceding event. In this case, the date but not the size of a future event can be estimated. (b) Slip-predictable model. Repeat times are proportional to the size of the future event. In this case, the size but not the time of the future event can be estimated.

American plates. The assessment of seismic potential is based on the level of conditional probability for recurrence in each zone as determined from the Weibull distribution analysis of the historic record. The degree of temporal resolution inherent in this approach is defined by the width or standard deviation of the observed density function, and is approximately 15% to 25% of the mean recurrence time. The Weibull distribution and associated probability and hazard functions are derived and more fully explained in Appendix A.

The second method for assessing seismic potential is somewhat more deterministic in nature and may be capable of providing more accurate estimates of recurrence times than do methods which treat earthquake recurrence as a purely stochastic process. Recent investigations of earthquake repeat times, both on global [Sykes and Quittmeyer, 1981] and regional [Bufe et al., 1977; Shimizaki and Nakata, 1980; Mogi, 1981] scales, suggest a simple model that describes both the physical and temporal aspects of the earthquake cycle along major plate boundaries (i.e., the time-predictable model of earthquake recurrence). As shown in Figure 1a, the time interval between two successive shocks, along the same segment of a plate boundary, is proportional to the displacement of the preceding earthquake, rather than the displacement of the shock that terminates the interval (i.e., the slip-predictable model of earthquake recurrence, Figure 1b). Both models define opposite ends of a spectrum of possible behaviors during the earthquake cycle. Observations of coastal uplift, tsunami wave heights and rupture lengths are compared from event to event to provide deterministic recurrence time estimates via the

2

TABLE 1. Conditional Probabilities (1984-2004)

Zone	Location, deg S	Last Shock	dT	Weibull Distribution Analysis, %			Deterministic Analysis			Poisson Analysis	
				All Data Mean=100 years	Zones 4, 5, and 6 Mean=87 years	Zones 3 and 7 Mean=126 years	T_{exp}	T/T_{exp} 1984-2004	F_s 1984-2004, %	T_{exp}	F_s 1984-2004, %
1	53-55	1949	35				70 175	0.500-0.786 0.200-0.314	22-28.4 0.005-0.7	70-175	11-25
2	46-55	No historic record									
3	37-46	1960	24	1.2-1.4		0.1-0.2	167	0.144-0.263	0.001-0.4	100-167	11-18
3A	37-39	1975	9	55-70 #			17	0.529-1.706	99-100	13-23	57-78
4	35-37	1939 1928	45 56	6.7-7.3 12.7-13.4	5.2-6.1 17-18		59 27	0.763-1.102 2.074-2.815	70.4-89.1 100	52-100 20-100	18-32 18-63
5	32-35	1906	78	32.7-33.1	72.2-74.8		79	0.987-1.240	76.2-95.8	79-100	18-22
6	30-32	1943	41	5.1-5.7	3.2-3.8		63	0.651-0.968	52.3-65.9	63-100	18-27
7	26-30	1922	62	17.2-17.7		4-5	104	0.596-0.788	21.2-24.3	100-126	15-18
8	25-27	1983 1966	1 18	39-61.4 # 50-55.3 #			12 22	0.083-1.750 0.818-1.727	99-100	10-22	46-86
9	18-24	1877	107	(66.4-69.3)	(100)	(31.4-32.4)	111 296	0.964-1.144 0.361-0.429	58.8-84.5 0.07-1.4	100-126	15-18
10	17-18	1868	116	(75.8-79.1)	(100)	(40.1-42.5)	111 296	1.045-1.225 0.392-0.459	65.6-90.9 0.13-1.8	100-126	15-18

Based on data from zones 3A and 8 only.
( ) Parentheses enclose values extrapolated from data in zones 3 through 7.

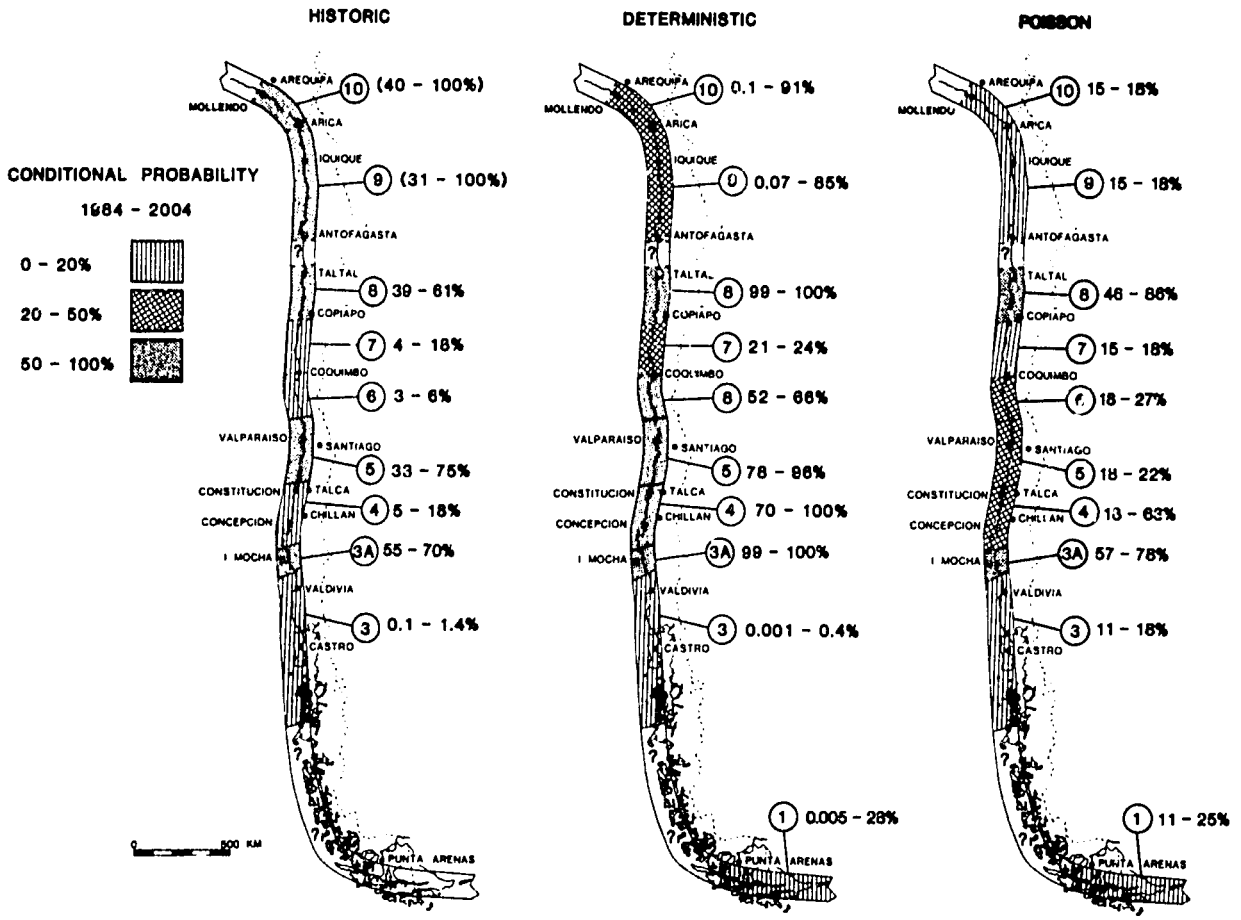

Fig. 2. Comparison of conditional probability estimates for large interplate earthquakes along the Chilean and southern Peruvian margins of South America: 1984-2004. Encircled numbers refer to the fault zones discussed in the text and listed in Table 1. The percentages beside each number represent the range of calculated probabilities for both historic (left side), deterministic (time-predictable) (center) and Poisson (right side) estimates. The numbers in parentheses for zones 9 and 10 are extrapolated values based on the Weibull analysis for central and southern Chile. The shading of each fault segment corresponds to the mean or preferred probability estimate. Blank areas denote the lack of sufficient historic data for analysis.

time-predictable model. More directly, estimates of the average displacement along the fault surface can be divided by the rate of fault motion to provide recurrence times. For older shocks, seismic moments and displacements can be determined, to within a factor of 2 or 3, using the estimated size of a particular rupture zone and various scaling laws [Sykes and Quittmeyer, 1981; Scholz, 1982].

The conditional probabilities of recurrence, based on the deterministic estimates presented in this study, are calculated on the assumption that the errors in recurrence time estimates are normally distributed about a mean value. As the data set for defining this distribution is small, distinguishing between a normally distributed error and some other type of distribution is difficult and the assumption of a normal or Gaussian distribution is used primarily as a numerical convenience. Input for each segment considered consists of the date of the last large shock, the estimated recurrence time and the width or standard deviation of the density function. A derivation and explanation are presented in Appendix B. In this method, the width or standard deviation of the normal distribution is estimated from the application of the aforementioned deterministic techniques to older shocks and ranges from 15% to 25% of the estimated recurrence time. As the time-predictable model is still a hypothesis, the probability estimates based on this model are presented as a test of the hypothesis. In addition, estimates via the time-predictable model can be compared and calibrated for those areas where historic data also exist.

The results of the above two methods are also compared to probability estimates based on a simple Poisson model of recurrence. The Poisson assumption (stationary earthquake occurrence which is random in the time domain) has been widely used and discussed by numerous authors as a basis for seismic hazards and risk analysis [Lomnitz, 1966; Cornell, 1968; Algermissen and Perkins, 1976; Rikitake, 1976b; Lomnitz and Nava, 1983]. An important consequence of the Poisson assumption is that the probability of failure is independent of the amount of time elapsed since the previous earthquake. This property of independence leads to conditional probabilities

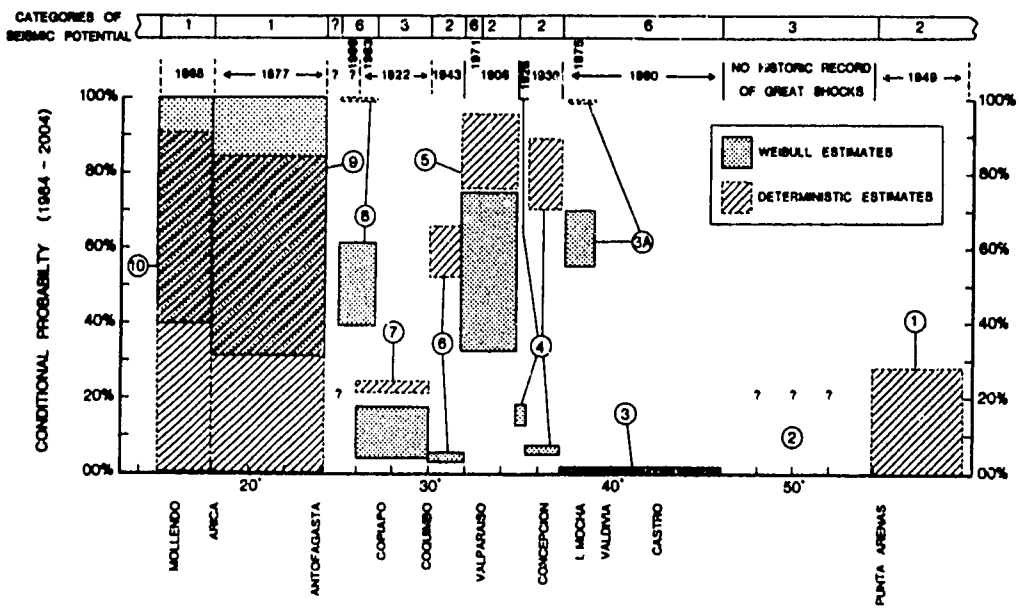

Fig. 3. Conditional probabilities for large earthquakes along the Chilean and southern Peruvian margins of South America: 1984-2004. Encircled numbers refer to the fault zones discussed in the text and listed in Table 1. For each segment, the height of the box represents the range of probabilities based on Weibull distributions (stippled boxes) and deterministic estimates (hachured boxes). Dates and arrows at the top of the graph are the time and lateral extent of the last large or great earthquake in each segment. The numbers at the top of the figure refer to the categories of seismic potential assigned to each segment according to the criteria of McCann et al. [1978, 1979] (category 1: T>100 years; category 2: 30<T<100 years; category 3: historic record incomplete; category 6: T<30 years; where T is the amount of time elapsed since the previous large or great shock).

which are static in time, and which are dramatically different from the time-varying probabilities in the two previous methods. The concept of static probability is also at odds with the basic seismic gap model which suggests that the probability for a future event grows with increasing time since the previous shock. The equations for conditional probability based on the Poisson assumption are presented in Appendix C. For the purposes of comparison, the frequencies of occurrence for the Poisson estimates of probability are taken from the mean or estimated repeat times determined by the Weibull and time-predictable analyses.

The types of analyses outlined above provide an important link between qualitative large-scale global studies (e.g., the maps of seismic potential by McCann et al. [1978, 1979] and Nishenko and McCann [1981]) and more refined estimates of recurrence based on intermediate and short-term precursory phenomena. Statistical analysis is also useful as a first step in assessing the potential of areas where the history of large shocks is poorly known. The extrapolation of repeat time information from adjacent segments may allow preliminary estimates of seismic potential, provided the tectonic regimes of both segments are similar.

Estimates of Seismic Potential

The following sections present and discuss the basic data for the 10 segments or zones along the transform and convergent margins of Chile and southern Peru considered in this study. The values of conditional probability calculated via the Weibull and deterministic analyses are summarized in Table 1 and Figures 2 and 3. Criteria for identifying the boundaries of each seismic zone and the larger seismic provinces in this analysis are (1) the ends of rupture zones of historic earthquakes as defined by intensity data, the extent of coastal uplift and aftershock distributions and (2) geologic and tectonic boundaries, such as major discontinuities in seafloor age; intersections of prominent bathymetric features on the Nazca plate with the continental margin; segmentations within the subducted Nazca plate, as defined by changes in the dip of the intermediate depth seismic zone; and associated geologic changes on the overriding plate such as the cessation of volcanism and changes in major structural trends [Barazangi and Isacks, 1976; Herron, 1981; Jordan et al., 1983]. In some areas, the boundaries are well defined, while in other areas they are more diffuse and poorly known.

The recognition of complex or multiple ruptures is an important factor in the interpretation of recurrence cycles. These are seismic zones with histories of one event in a previous cycle and two or three smaller events in the following cycle. A recent example of this type of behavior occurred in the Columbia-Ecuador seismic zone, which was entirely ruptured by a great shock in 1906 and subsequently reruptured by a series of smaller events in 1941, 1958 and 1979 [Kanamori and McNally, 1982; Mendoza and Dewey, 1984]. For these areas, the repeat time is taken as the time between the larger, previous

5

shock and each of the individual smaller shocks rather than the time between each subsequent shock.

Stochastic Estimates of Seismic Potential: Average Repeat Times and Weibull Distributions

One simple and straightforward method to estimate earthquake recurrence dates is the use of average repeat times for any one segment or segments of a plate boundary. Recurrence date estimates based on average repeat times for those areas along the Chilean-southern Peruvian margin with a history of three or more large shocks (i.e., two or more repeat intervals), however, are only available for half of the margin. Other segments have histories of only one or two large shocks (e.g., southern Peru-northern Chile, zones 9 and 10) or no history of large earthquakes at all (e.g., southern Chile, zone 2). For those areas with a long enough history, the temporal resolution of the average repeat time approach can be evaluated using the ratio T/T_{ave}, where T is the actual repeat time and T_{ave} is the average repeat time for each individual segment or rupture zone. This ratio gives an estimate of the uncertainty in terms of a fraction or percentage of repeat time rather than in absolute years. This approach will be used again, later in this study, to provide a constraint on the degree of temporal resolution for the deterministic estimates of recurrence time. In Figure 4a the ratio T/T_{ave} is calculated for all of the historic shocks of central and southern Chile that were used in this study. Overall, for the majority of large shocks, the average recurrence estimate works reasonably well ($2\sigma=\pm28\%$ of the average repeat time in Figure 4a) and is a suitable first step for long-term forecasting. The tightness of the clustering of T/T_{ave} values around 1.0 in Figure 4a primarily indicates that the majority of rupture zones sampled have relatively periodic repeat times with small standard deviations. This suggests that many segments may be characterized as having relatively constant strain rates and source properties from event to event.

A more robust approach for statistically estimating seismic potential is possible by making use of Weibull distributions (as described in Appendix A). Figure 5 shows the basic data set used in the analysis of Chilean shocks. The frequency histogram of observed recurrence times in Figure 5a is composed entirely of the repeat times of large and great underthrust shocks that have occurred in the region from 26° to 46°S. Figure 5b shows the least squares fit to the reliability-recurrence time relationship. When all the data in Figure 5a are plotted, the resulting fit is well described by the two-parameter Weibull model (r, the linear correlation coefficient=0.925; β, the slope of the best fit line=4.82; mean repeat time=100 years; and the results of the Mann test for lack of fit to the two-parameter Weibull model are not significant at the 95% or 90% confidence levels, S=0.66, see Appendix A). While the data in Figure 5b are well described by a single straight line fit, there is an indication of a change in slope or recurrence time behavior at T=100 years (ln t=4.6). In Figure 5c, the data have been divided

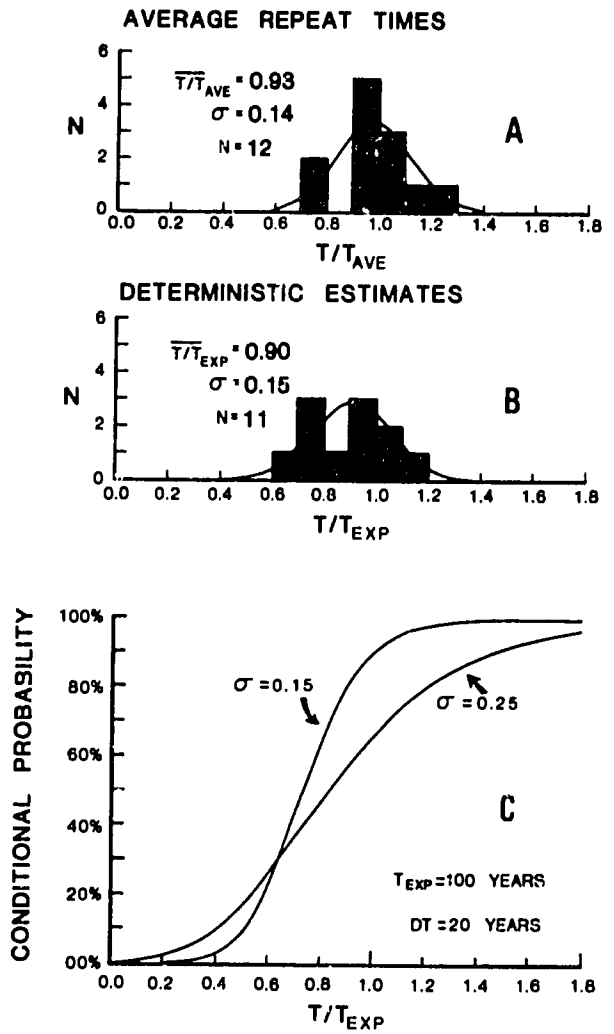

Fig. 4. Histograms of T/T_{ave} and T/T_{exp} values and conditional probability curves. (a) Values of T/T_{ave} based on average repeat times for each individual segment of the Chilean margin (see Table 2). In this case, T is the actual repeat time and T_{ave} is the average recurrence time for events in each segment. The mean value of T/T_{ave}, assuming the data fit a normal distribution, is 0.98 ± 0.14 ($\pm1\sigma$). N is the sample size. (b) Values of T/T_{exp} based on deterministic estimates of repeat time. T_{exp} is the estimated recurrence date for a set of historic Chilean shocks listed in Table 2 and T is the actual recurrence time. T/T_{exp} values are assumed to be normally distributed around a mean value; in this case $T/T_{exp}=0.90\pm0.15$ ($\pm1\sigma$). (c) Conditional probability curves for a sample case with $T_{exp}=100$ years, dt =20 years and $\sigma=0.15\%$ and 0.25% (15 and 25 years) are shown based on the function in Figure 4b.

into two subsets (those zones with repeat times less than 100 years (zones 4, 5 and 6), and those zones with repeat times greater than 100 years (zones 3 and 7)).

Although the data are few, there appear to be two types of recurrence behavior along the Chilean margin. As seen by the variation of the shape parameter β in Figures 5b and 5c, one pattern is typified by a small variance and repeat

6

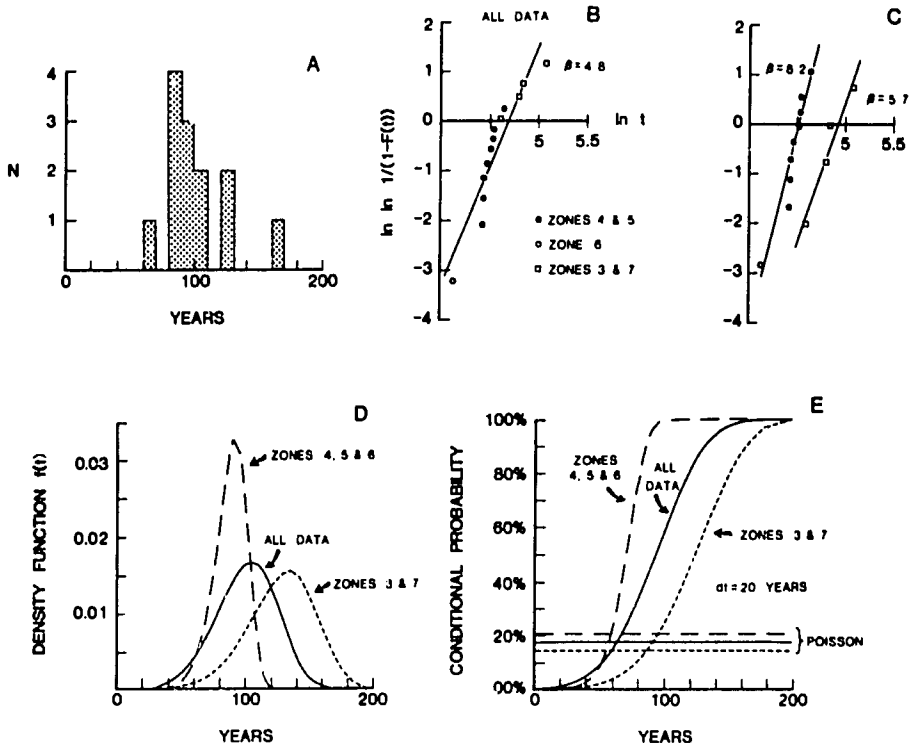

Fig. 5. Weibull distribution analysis of great earthquake recurrence times along the Chilean margin 26°-46°S. (a) Frequency histogram of observed recurrence times (listed in Table 2). Note that the distribution is asymmetric and not well described by a normal distribution. (b) A plot of ln ln (1/1-F(t)) as a function of ln t for the repeat times in Figure 5a. A least squares fit to the data defines the parameters for the Weibull reliability or survivor equation, R(t), with β=4.8 and k=7.40 X 10^{-10}. Symbols denote data from individual segments. Note that while the data are satisfied by the single straight line, there appears to be a change in slope and repeat time behavior at ln t=4.6 (100 years). (c) The data in Figure 5b are grouped by zone into those areas with repeat times less than and greater than 100 years (zones 4, 5 and 6 and zones 3 and 7, respectively). The values of β are 8.2 and 5.7, and k values are 6.65 X 10^{-16} and 3.63 X 10^{-12} respectively. The segregation suggested by the change in slope is also substantiated by the observation that both groups correspond to different tectonic regimes. (d) Density function curves [f(t)] for all the data in Figure 5a and the two subgroups of data suggested by the analysis in Figure 5b. (e) Conditional probability curves (dt=20 years) based on the density function curves in Figure 5d. For comparison, the horizontal lines labeled Poisson are conditional probabilities for 20-year time increments assuming a Poisson distribution and the same mean recurrence times determined in Figures 5b and 5c.

times less than 100 years (zones 4, 5 and 6; mean repeat time=87 years), while the other has a larger variance and repeat times greater than 100 years (zones 3 and 7; mean repeat time=126 years). The apparent change in recurrence time behavior at about 100 years appears to coincide with along-strike variations in the megatectonic regime of the Chilean subduction zone. Zone 3 (38°-46°S) is associated with a shallow dipping subduction zone and a wide interface, the subduction of relatively young seafloor (<20 m.y.) and a history of large ruptures. To the north, zones 4 and 5 are associated with a steeper dipping subduction zone, a narrower interface, the subduction of older seafloor (>30 m.y.), and smaller ruptures. In contrast, zone 7 (26°-30°S) also has a history of great shocks with large rupture dimensions and is associated with that segment of the Chilean margin that has an absence of Quaternary volcanism and a shallow intermediate depth seismic zone.

Figure 5d shows the resulting probability density functions f(t), calculated from the least squares fits in Figures 5b and 5c. The standard deviation or width of the density function corresponds to the degree of temporal resolution, and decreases as β increases. For the three β estimates in Figures 5b and 5c (8.2, 5.7 and 4.8), σ=15%, 24% and 24% of the mean recurrence time, respectively. In Figure 5e, the conditional probability curves represent the probability of occurrence within a specified time interval, T+Δt, (in this case, Δt=20 years), provided the earthquake in question does not occur prior to T. The three probability curves show the variation of conditional probability with time as a function of changes in β. To illustrate the basic contrast between the Poisson and Weibull models, Figure 5e also shows the Poisson probabilities using the same mean repeat times found in Figures 5b and 5c. The Weibull-based conditional probabilities are time-dependent, whereas

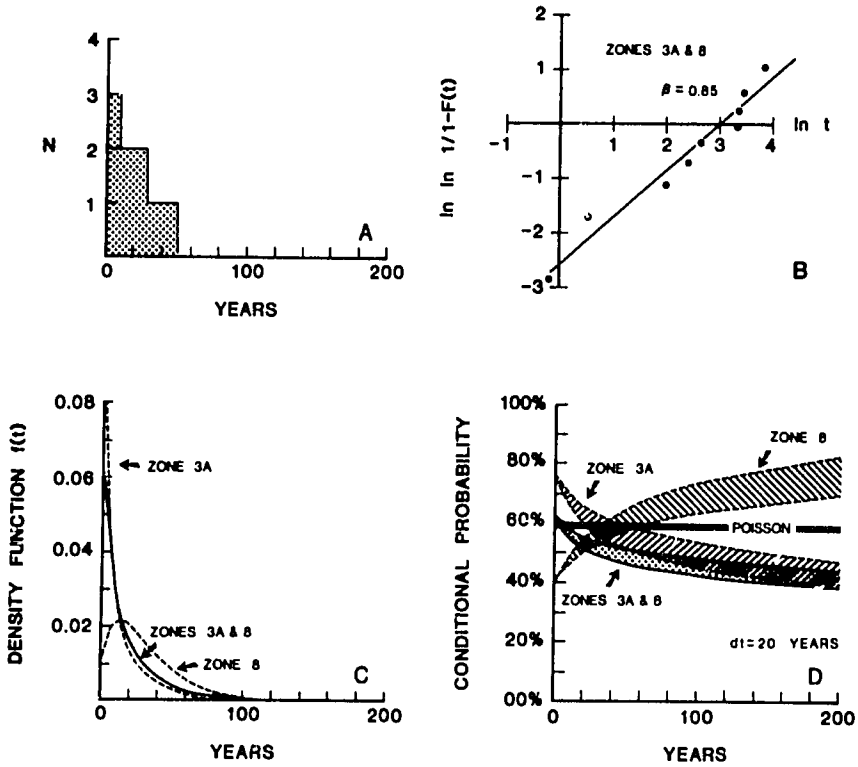

Fig. 6. Weibull distribution analysis of large earthquake recurrence times for zones 3A and 8. (a) Frequency histogram of observed recurrence times in both zones. (b) A plot of ln ln (1/1-F(t)) as a function of ln t for the combined repeat times in zones 3A and 8; β=0.85, k=0.065. (c) Density functions based on least squares fit in Figure 6b (solid line) and for each individual zone (dashed lines). (d) Conditional probability curves (dt=20 years). The hachured and stippled areas between the curves illustrate the possible range in probability estimates as a function of the two plotting rules discussed in Appendix A. Note the relatively constant level of probability with time when compared with the time-varying probabilities in Figure 5e. For comparison, the Poisson estimate of conditional probability is also shown.

the Poisson-based conditional probabilities are time-independent. In this analysis, the Weibull probability estimates for each zone (see Figures 2 and 3 and Table 1) are calculated using the mean repeat times and the parameters from the least squares fits in Figures 5b and 5c, where applicable.

In addition to analyzing the recurrence behavior of great earthquakes, the above techniques are also applied to two smaller zones with histories of large shocks (7<M<8). Both the Mocha Island block (zone 3A) and the Copiapo-Taltal region (zone 8) have a high concentration of large (M>7) shocks during this century when compared to adjacent segments of the Chilean margin. Figure 6a shows a histogram of recurrence times from both zones. As the size of each of the two zones is larger than any single rupture, a bias toward shorter repeat times is possible (i.e., the time between adjacent ruptures being counted as a repeat rather than the time between overlapping ruptures). Figure 6b shows the least squares fit of the data from both zones to the Weibull reliability-recurrence time relationship. The shape parameter β in this case is smaller than the values of β in Figure 5. The resulting density function (solid line in Figure 6c) is close to an exponential distribution (β=1.0). For zone 3A alone, β=0.76; for zone 8 alone, β=1.4 and for both zones, β=0.85. The consequence of this type of distribution is that the hazard rate and conditional probabilities become relatively constant, when viewed in 20-year increments (see Figure 6d). In this case, the Poisson model of recurrence (β=1) appears to be a more appropriate representation as shown in Figure 6d. Both of these areas appear to be associated with major tectonic boundaries or segmentations along the Chilean margin, and these inhomogeneities may be acting as asperities which tend to fail more frequently than those in adjacent zones.

The application of the conditional probability curves in Figures 5e and 6d to the seismic zones along the Chilean and southern Peruvian margins is shown in Figures 2 and 3 and Table 1 for the time span 1984-2004. For comparison, the date of the last large or great shock and the corresponding seismic potential designations of McCann et al. [1978, 1979] are shown at the top of Figure 3. In general, both the qualitative seismic potential designations and the Weibull probability estimates are in good agreement. For example, zone 3, which last ruptured in 1960, is assigned to category 6 and has a low probability (<2%) of recurrence during the next 20 years. In contrast, the Big Bend region of South America (northern Chile and southern Peru, zones 9 and 10) was the site of two great shocks in 1868 and 1877 (M_t=9.0, [Abe, 1979]) which produced

destructive Pacific-wide tsunamis and is assigned to category 1. This region has an intermediate to high level of probability (31-100%). In this case, however, care must be taken not to interpret the data too literally, as these results are based on the extrapolation of recurrence behavior from southern and central Chile. The only great tsunamigenic shock in this region prior to 1868-1877 occurred near Arica in 1604 (a 264-year repeat time). Incomplete historic records, and variations in population density, make it difficult to assess whether a 264-year recurrence time is characteristic of this region, or the result of an incomplete historic record. Spatial variations in tectonic regimes, the amount of aseismic slip, convergence directions, etc., may make these segments vastly different from other segments of the Chilean margin. Hence, the actual seismic potential may be higher or lower than shown for zones 9 and 10 and in general is poorly constrained. Of the segments assigned to category 2 by McCann et al. [1978, 1979], the Valparaiso region (zone 5) which last ruptured in 1906, clearly has the highest conditional probability for recurrence during the next 20 years (33-75%). In this case, the zone is within a segment of the Chilean margin where historic shocks are well documented. Hence there is greater confidence in the higher level of probability (72-75%; see Table 1) which is based on data from this zone. The average recurrence time for great shocks in this zone is 86±10 years. In addition, there are observations of coastal uplift for two previous Valparaiso earthquakes (1822 and 1906) which enable deterministic estimates of a recurrence time. These data allow for an independent evaluation of the level of seismic potential and will be discussed in the next section.

Deterministic Estimates of Seismic Potential

The following sections discuss recurrence time estimates for the 10 seismic zones along the Chilean and southern Peruvian margin from a deterministic standpoint and use the time-predictable model of earthquake recurrence as a working hypothesis. The size and recurrence times of previous large and great earthquakes are compared using estimates of source size as inferred from scaling laws and instrumental observations, far-field tsunami heights and the amounts and extent of coseismic coastal uplift. These data are summarized in Table 2. An important simplifying factor in this analysis is that the relative convergence vector between the Nazca and South American plates is nearly constant in magnitude and direction along the Chilean margin. This consistency is the basis of my extrapolation of the Weibull distributions from one segment of the margin to another and of my postulating a correlation of varying repeat time behavior with changes in tectonic regime. The presence of aseismic slip, which serves to decrease the amount of relative convergence that is partitioned in seismic strain buildup [Kanamori, 1977b; Sykes and Quittmeyer, 1981], is an important but poorly understood parameter in recurrence calculations. In this study, the effect of aseismic slip is accounted for by multiplying the convergence rate by the term α (the ratio of seismic to total slip or convergence). Estimates of recurrence that are based on dividing the displacement in a previous shock by the total convergence rate, ignoring the effects of aseismic slip, would tend to underestimate the recurrence time and overestimate the resulting conditional probability. Repeat times derived from various deterministic lines of argument are used to constrain an average recurrence time which is used in conjunction with a normal distribution function (with width or standard deviation equal to 15% to 25% of the recurrence time) to estimate the level of conditional probability for each zone during the next 20 years, 1984-2004.

Zone 1: Punta Arenas - Tierra del Fuego, 52°-55°S

The earliest large earthquake that is documented for this region occurred on February 2, 1879. Intensities reached Modified Mercalli (MM) VII in Punta Arenas and MM VIII (?) in Tierra del Fuego [Lomnitz, 1970]. Few details are known otherwise. On December 17, 1949 two events (M_s7.7) occurred within 8 hours of each other. The intensity of the second shock was around MM VII in Punta Arenas [Lomnitz, 1970]. Although the epicenters of both events are poorly determined, field investigations by Winslow [1982] associate both events with the Magellan fault of Katz [1964], and the transform plate boundary between the South American and Scotian plates. Offsets associated with these two events extend from the western end of the Brunswick Peninsula (near Punta Arenas) to Policarpo (Tierra del Fuego) [Winslow, 1982 and personal communication, 1982], and suggest a fault length of about 450 km.

If we assume the two events in 1949 had equal rupture dimensions (about 225 km), the estimated displacements based on scaling laws, range from 280 to 423 cm. Dividing these estimates by the rate of fault motion in the area (about 2 cm/yr) gives estimated recurrence times of 140 to 211 years, or 2 to 3 times the observed recurrence time (70 years). In view of the extreme variation of these estimates and the uncertainty in the rate of fault motion, a quantitative description of seismic potential in this area is difficult. The estimates of repeat time are based on displacement and seismic moment estimates which are in reasonable agreement with the assigned magnitude of M_s=7.7. The average of these estimates (140 and 211 years) is 175 years and the conditional probability during the next 20 years is less than 1%. Under the Poisson assumption the conditional probability is 11%. If the 70-year repeat time from the historic record is more characteristic for this segment, the resulting conditional probability for the next 20 years increases to 22-28.4% or 25% under the Poisson assumption. In spite of these low estimates, more work is needed in this region to accurately document the seismic history.

Zone 2: Chile Rise Intersection - Straits of Magellan, 46°-52°S

South of the intersection of the Chile Rise with the South American plate at 46°S, the

TABLE 2. Source Parameter

Zone	Average Repeat Time, years ±2σ	Date	Length,[a] km	Width,[a] km	Displacement,[a] m	Mo,[a] x10^{27} dyne cm	Magnitude[b,c]
1		Dec. 17, 1949	450	20	2.8-4.2[f]	2.8-4.2	7.7[b]
		Feb. 2, 1879					
2		No historic record of large or great shocks					
3		May 22, 1960	1000	210	19	2000[h]	9.4[c]
		Nov. 7, 1837	(700-750)	(200)	(13-15)	(900-1000)	9.25[c]
	128±62	Dec. 24, 1737	(700-750)	(200)	(13-15)	(900-1000)	(9.2)
		Dec. 16, 1575	(1000)	(210)	(19)	(2000)	(9.4)
3A	13±10	May 10, 1975			1.2-1.7[1]	2.8[1]	7.6[b]
		June 20, 1960			0.8-1.2[1]	0.84[1]	7.25
		April 20, 1949			0.9-1.2[1]	1[1]	7.3
4		Jan. 25, 1939	(200)	(100)	(4)	35	8.3
	92±15	Dec. 1, 1928	(88)	(88)	(1.7-2)	1.5-3	7.9
		Feb. 20, 1835	(400)	(150)	(6.7-8)	160-192	
		May 25, 1751					
		March 15, 1657					
		Feb. 8, 1570					
5		Aug. 16, 1906	330	(100-150)	3-6	29-50	8.4[c]
	86±10	Nov. 19, 1822	(330)	(100-150)	(3-6)		
		July 8, 1730	(350-450)	(100-150)	(6-8)		
		May 13, 1647					
6		April 6, 1943	(150-250)	(100-150)	(2.8-5.4)	25	8.2[c]
		Aug. 15, 1880	(150-250)	(100-150)	(2.8-5.4)	(25)	(8.2)
		July 8, 1730					
7		Nov. 10, 1922	(330-450)	(150-200)	(6-11)	(130-300)	8.2-8.7[b,c]
		March 30,1796			(6-11?)		
8		Oct. 4, 1983			(0.9-1.2)[1]	1[1]	7.3
		Aug. 3, 1978			(0.6-0.8)[1]	0.35[1]	7.0
		Aug. 2, 1946			(1.7-2.3)[1]	(7.9)[1]	7.9
		Dec. 28, 1966			1.4-2.5[1]	4	7.7[b]
9		May 9, 1877	(450-650)	(150)	(8-12)	300-400	9.0[c]
10		Aug. 13, 1868	(300-400?)	(150)	(8-12)	300-400	9.0[c]

[a]Source parameters in parentheses estimated from intensity and aftershock data [Lomnitz, 1970; Kelleher, 1972] and scaling laws [Sykes and Quittmeyer, 1981; Scholz, 1982].
[b]Magnitude estimate: M_s [Abe, 1981, 1983].
[c]Magnitude estimate: M_t [Abe, 1979].
[d]Recurrence estimate in years: $T_{R2} = [U_2/U_1]^p\ T_{R1}$, p = 1.0 and 0.75, U = displacement.
[e]Recurrence estimate in years: $T_{R2} = [L_2/L_1]^p\ T_{R1}$, p = 1.0 and 0.75, L = length.
[f]Calculations based on two events with equal rupture lengths (~225 km).
[g]Repeat time if 1949 sequence similar to 1879 event.
[h]Source parameters from Sykes and Quittmeyer [1981].
[i]α = ratio of seismic/total slip = 1.00.
[j]Based on 1960-1837 event pair for calibration.
[k]Repeat time based on ratio of 1837 and 1960 tsunamis.

10

and Recurrence Time Estimates

Displacement/ Convergence Rate, years	T/T_{exp}	Ratio of Displacements,[d] years	T/T_{exp}	Ratio of Lengths,[e] years	T/T_{exp}	Other Estimates	Average T_{exp}
140-211[i]						70[g]	70-175
211[i]		147-180[j]		152-175[j]			167
144-167[i]	0.74-0.85					160[k]	
144-167[i]	0.60-0.69	123[j]	0.81	123[j]	0.81		
211[i]	0.77	147-180[j]	0.90-1.10	152-175[j]	0.93-1.06		
14-19[i]							17
10-13[i]	1.15-1.50						
10-14[i]	0.78-1.10						
54[m]		52-70[n]		52-62[n]			59
23-27[m]		20-37[n]		20-30[n]			27
91-108[m]	0.86-1.15						
58-117[o]				84[p]		57[q]	79
58-117[o]	0.72-1.45			67-88[r]	0.80-0.96		
104-117[o]	0.78-0.88						
		63[s]		63[s]			63
74-135[t]							104
104	1.21						
10-13[i]							12
7-9[i]	0.50-0.71						
19-26[i]	1.23-1.69						
16-28[i]							22
88-133[i]							111
148-444[u]							296
88-133[i]							111
148-444[u]							296

[l]Source parameters based on moment/magnitude and magnitude/area relations [Kanamori and Anderson, 1975; Kanamori, 1977a].
[m]$\alpha = 0.82$.
[n]Based on 1835-1928, 1939 event pairs for calibration.
[o]$\alpha = 0.70$.
[p]Repeat time if 1906 event similar to 1822 event.
[q]Repeat time based on ratio of coseismic coastal uplift in 1822 and 1906.
[r]Based on 1730-1822 event pair for calibration.
[s]Repeat time if 1880 and 1943 events similar in size.
[t]$\alpha = 0.90$.
[u]$\alpha = 0.30-0.60$.

Antarctic plate is being subducted beneath the west coast of South America and the convergence rates decrease from 9 cm/yr (NAZ-SAM) to about 2 cm/yr (ANT-SAM) [Forsyth, 1975; Minster and Jordan, 1978]. The continental margin is characterized by sediment-filled trench [Ewing et al., 1969], a low level of seismicity and no history of great earthquakes [McCann et al., 1978, 1979]. The region from 46° to 49°S is also associated with a gap in recent volcanism and corresponds to that segment of the Chilean margin where the Chile Rise was subducted between 6 and 2.5 m.y. ago [Herron et al., 1981]. This region was originally classified by McCann et al. [1978, 1979] into category 5 (no historic record and may not have potential for great shocks). Nishenko and McCann [1981] took a more conservative approach and revised the classification to category 3 (historic record incomplete, but may have the potential for a great earthquake). In view of the low convergence rate, repeat times for large and great shocks in this region may be a few hundred years. At present, however, no data are available to estimate a recurrence time.

Zone 3: Mocha Island Block - Chile Rise Intersection, 38°-46°S

Previous great earthquakes that have ruptured this segment of the Chilean margin occurred in 1575, 1737, 1837 and 1960 and all are estimated to have rupture lengths between 700 and 1000 km. The average repeat time is 128±62 years (±2σ), assuming that no events have been unreported during this time. The boundaries of this seismic zone are defined by the intersection of the Chile Rise with the Chilean margin at 46°S and by the Mocha Island block at 38°-39°S. The former feature primarily acts as a barrier for the propagation of large shocks to the south (i.e., into zone 2) as pointed out by Mogi [1969] and Aki [1979], while the latter is an active area for large shocks and will be discussed separately as zone 3A.

The great 1960 event (M_w9.5) comprised a series of multiple ruptures which started in the Mocha Island block on May 21 and continued south to the Chile Rise on May 22 [Saint-Amand, 1963; Plafker and Savage, 1970; Nagume, 1971]. Assuming that the amount of aseismic slip in this zone is negligible (i.e., α=1.0 [Sykes and Quittmeyer, 1981]), the average displacement (1900 cm) divided by the convergence rate (9 cm/yr) gives an estimated recurrence time of 211 years, which is longer than the observed recurrence times for this zone. Fortunately, other data can be used to evaluate this recurrence time estimate.

The November 7, 1837, shock (M_t9.25) followed 2 years after the 1835 Concepcion shock, which ruptured the adjacent seismic zone to the north (zone 4). The rupture length in 1837 appears to be significantly smaller than the 1960 shock (as the 1835 event ruptured the Mocha Island block and an unknown distance south (see Figure 7)), and is estimated to extend from the latitude of Valdivia (40°S) to the Chile Rise (46°S), approximately 700 km. The southern limit is constrained by observations of uplift associated with the 1837 shock at Lemu Island (45.17°S; about 2.4m) [Darwin, 1851]. Use of the ratio of lengths of the 1960 and 1837 shocks as a parameter for constraining the next recurrence time gives estimates of 150 to 175 years (see Table 2).

Sykes and Quittmeyer [1981] suggest that tsunami height is proportional to seismic moment, so the ratios of both quantities should be approximately equivalent, but probably uncertain to at least a factor of 2. Tsunami heights at Hilo, Hawaii, for the 1960 and 1837 events are 10.5 and 6.0 m, respectively [Iida et al., 1967], and the ratio of tsunami heights is 0.57. Assuming that the rigidities and widths of both earthquakes are similar, the calculated displacement U in the 1837 shock is 1444 cm, given by

$$\frac{M_{o_{1837}}}{M_{o_{1960}}} = 0.57 = \frac{750\text{km } U_{1837}}{1000\text{km } 1900\text{cm}}$$

which is in good agreement with the displacement estimates based on scaling laws (Table 2). The estimated recurrence time T_{exp} for the 1837 shock ranges from 144 to 167 years, using a displacement of 1300-1500 cm divided by the convergence rate. The actual repeat time T is 123 years and the ratio T/T_{exp}=0.74-0.85.

Few details are known about the great shock on December 24, 1737. Assuming that the source parameters for the 1737 event are similar to the 1837 event, the estimated recurrence time based on average displacement divided by the convergence rate is 155 years and T/T_{exp}=0.65. Using the ratios of displacements and lengths, with the 1837-1960 pair as a calibration, gives a repeat time of 123 years and T/T_{exp}=0.81. The long recurrence time between the December 16, 1575, and 1737 shocks (162 years) suggests that the 1575 shock was similar in size to the 1960 event, assuming no great shocks occurred and were unreported during the time interval 1575 to 1737. In addition, Lomnitz [1970] states that the description and extent of damages associated with the 1575 shock are similar to those of the 1960 shock. Using the displacement in 1960, the estimated recurrence time is 211 years and T/T_{exp}=0.77. Using the ratio of displacements and the 1837-1960 pair as a calibration, the recurrence time estimates range from 147 to 180 years and the ratio T/T_{exp} ranges from 0.90 to 1.10 (see Table 2).

In summary, estimates for the recurrence time of the next great southern Chilean earthquake are listed in Table 2, and range from 147 to 211 years. Using the average recurrence time estimate of 167 years, the conditional probability for recurrence during the next 20 years ranges from 0.001% to 0.4% and compares favorably with the Weibull estimates of 0.1% to 1.4% for the same time interval. In contrast, the estimate of conditional probability under a Poisson assumption is 11% (see Figures 2 and 3).

Zone 3A: Mocha Island Block, 37.5°-39.5°S

Mocha Island (38.2°S) is situated on a crustal block that overrides a boundary zone between two tectonic regimes in the subducted Nazca plate [Herron, 1981]. South of 40°S, the seafloor at the Chile trench is of anomaly 5E age (18 m.y. B.P.) and younger and was formed at the presently active East Pacific Rise. Seafloor to the north

12

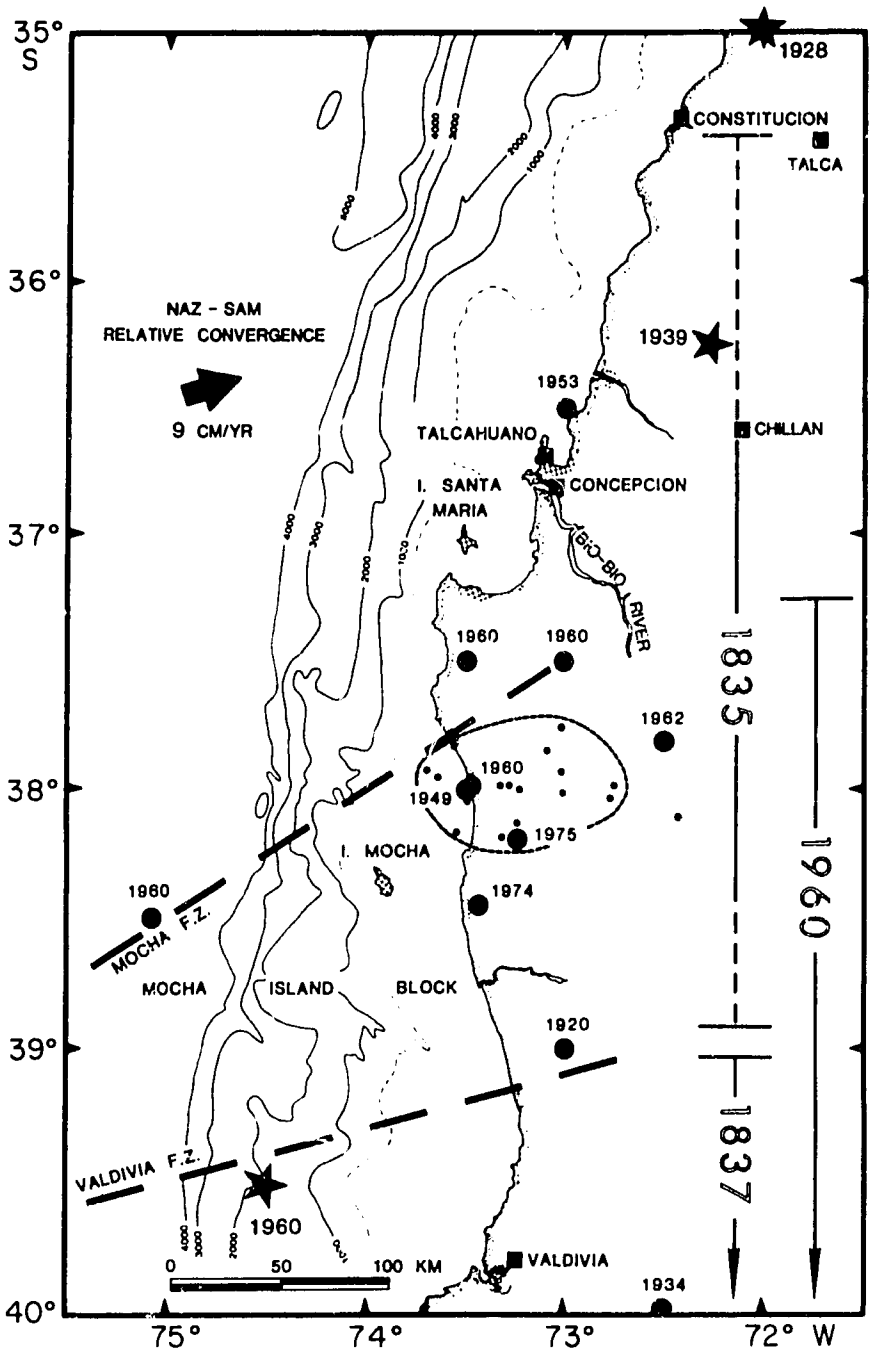

Fig. 7. Recent and historic earthquakes in the Concepcion area. Coastal outline and bathymetry (contour interval 1000 m) from Prince et al. [1980]. Projection of the Mocha and Valdivia Fracture Zones from Herron [1981]. Epicenters from Gutenberg and Richter [1954] and the International Seismological Centre (ISC) Bulletin. Location of aftershocks associated with the 1975 (M_s7.5) event from the ISC Bulletin. Hachured segments of the coast are areas of observed coastal uplift following the 1835 Concepcion shock [Darwin, 1851] and include Mocha Island, Santa Maria Island and the Talcahuano-Concepcion areas. Rupture dimensions for great shocks in this area (1835, 1837 and 1960) are solid where known and dashed where inferred. The northern extent of the 1960 rupture is from Plafker and Savage [1970]. Note the apparent overlap between the 1835 and 1960 rupture zones in the vicinity of the Mocha Island block. Most of the seismicity (M>7) in this area is concentrated near the projection of the Mocha Fracture Zone, which is judged to have a nearly constant hazard rate.

of the Mocha Island block was formed by the now extinct Pacific-Farallon spreading center [Handschumacher, 1976; Herron, 1981]. The geometry of the interplate boundary changes orientation in this area; to the south it is flatter and wider than the zone to the north [Kadinsky-Cade and Isacks, 1983]. The change in the geometry of the interplate boundary is also marked by a westward shift in the location of shallow seismicity and an absence of intermediate and deep hypocenters

in zone 3 when compared to zone 4 [Barazangi and Isacks, 1976; Herron, 1981]. Zone 3A also has a level of background seismicity that is higher than adjacent segments of the Chilean margin. R. Habermann and W. McCann [manuscript in preparation, 1984] suggest that this increased activity is related to the subduction of a segment of the inactive Pacific-Farallon spreading center beneath the margin.

In addition to being involved in the great earthquakes which occur in this region, the Mocha Island block has independently produced a number of large (7<M<8) shocks during this century. The majority of these shocks, including the foreshocks to the great 1960 event, are located near the projection of the Mocha Fracture Zone (see Figure 7). The occurrence of events in 1920, 1949, 1960-1962 and 1974-1975 indicates an average recurrence time of 13.2 ±10 years, which is approximately 10% of the recurrence time for great shocks (M>8) in this area. The estimated displacement of the 1975 (M_s7.6) shock is about 120-170 cm and the corresponding recurrence time ranges from 14 to 19 years, implying a conditional probability of 99-100% for a large earthquake during the next 20 years. For comparison, the Weibull estimates of probability for this area (see Figure 6 and Table 1) range from 55% to 70%, and the Poisson estimates range from 57% to 78%.

Zone 4: Constitucion - Concepcion, 35°-37°S

Previous great earthquakes in this zone occurred in 1570, 1657, 1751, 1835 and 1928-1939. The average repeat time is 92.4±15 years (±2σ), and the small standard deviation would suggest that large earthquakes in this region are fairly periodic and near constant in size. The boundaries of this zone are well defined to the south by the Mocha Fracture Zone and the northern limit of the 1960 break, and to the north by the southern extent of the 1906 rupture in zone 5. While the Mocha Fracture Zone corresponds to a major tectonic discontinuity between zones 3 and 4, no similar features are apparent between zones 4 and 5.

When the December 1, 1928 (M7.9) and the January 25, 1939 (M8.3) events are compared to the preceding shock of February 20, 1835, the twentieth century series of shocks appear to be smaller and may be followed by shorter recurrence times (and hence, have higher probabilities of recurrence than indicated by the Weibull analysis of the historic record). Reports of coastal uplift associated with the 1835 event firmly constrain the rupture zone from the Talcahuano-Concepcion region (36.5°S) to Mocha Island (38.2°S) [Darwin, 1851]. Supplementary evidence suggests a rupture from Constitucion (35.3°S) [Caldcleugh, 1836] to north of Valdivia (39°S) for a rupture length of about 400 km (see Figure 7). In contrast, the 1928 Talca event has an estimated rupture dimension of approximately 80-90 km [Kelleher, 1972], and it is unclear whether this event represents a smaller, simple plate boundary type of earthquake or is an intraplate event (either in the overriding crust or the subducted Nazca plate). The intensity pattern of the 1928 shock trends east-west [Bobillier, 1930] instead of north-south as do other underthrust events. The 1965 Aconcagua earthquake in zone 5 also exhibited an east-west pattern of intensities and was a normal faulting earthquake within the subducted Nazca plate [Malgrange et al., 1981]. It is not known whether the east-west pattern of isoseismals in 1928 reflects population density along a river valley or a different faulting mechanism, as this event produced coastal uplift at Putu (35.1°S) [Lomnitz, 1970]. The 1939 Chillan event also had a smaller rupture zone than the 1835 event, as the former did not rupture the Mocha Island block (zone 3A) and apparently only ruptured the deeper portion of the plate interface. This interpretation is suggested by the lack of both a tsunami and any appreciable coastal uplift [Saita, 1940]. A smaller shock occurred updip of the 1939 event on May 6, 1953 (M_s7.6; see Figure 7), which may have ruptured the shallow portion of the plate interface and completed the rupture process started in 1939.

The ratios of length and displacement for the 1835 and 1928-1939 shocks indicate repeat times of 20 to 37 years for the 1928 zone and 52 to 70 years for the 1939 zone (see Table 2). As a somewhat independent constraint on the recurrence time of the 1939 shock, Lomnitz [1970] notes that the extent of the region of damage associated with the 1939 shock is similar to the 1943 Illapel shock (zone 6), which also has an estimated recurrence time of about 60 years. Directly dividing the displacements in 1835 (670-800 cm) by 9 cm/yr gives a repeat time of 75 to 89 years. These times are in general agreement, but slightly shorter than the observed recurrence times of 93 to 104 years. If this discrepancy is related to aseismic slip, rather than errors in the use of scaling laws, I estimate α (the ratio of seismic to total slip) to be about 0.80 by dividing the above displacements by an average repeat time of 98 years. Using an α of 0.80, and the estimated sizes of the 1928 and 1939 events, the recurrence time estimates range from 23 to 27 years for the 1928 zone and 54 years for the 1939 zone.

In summary, estimates for the recurrence time of large shocks in zone 4 range from 20 to 37 years and 52 to 70 years for the 1928 and 1939 ruptures, respectively. The corresponding conditional probabilities range from 100% for the 1928 zone to 70% to 89% for the 1939 zone and are significantly higher than those calculated from the historic record using Weibull distributions (5-18%; see Table 1). For comparison, the conditional probabilities for the 1928 and 1939 zones under a Poisson assumption range from 42% to 63% and 25% to 32%, respectively.

Zone 5: Los Vilos - Valparaiso - Constitucion, 32°-35°S

Previous earthquakes in this seismic zone occurred in 1647, 1730, 1822 and 1906. The average repeat time is 86±10 years (±2σ). The boundaries of this zone are based primarily on the rupture dimensions of the 1906 shock, as determined from uplift data (see Figure 8). This zone straddles a major tectonic boundary: the intersection of the Juan Fernandez Islands with the Chilean margin at 33°S. Within the trench, this intersection is marked by an increase in the

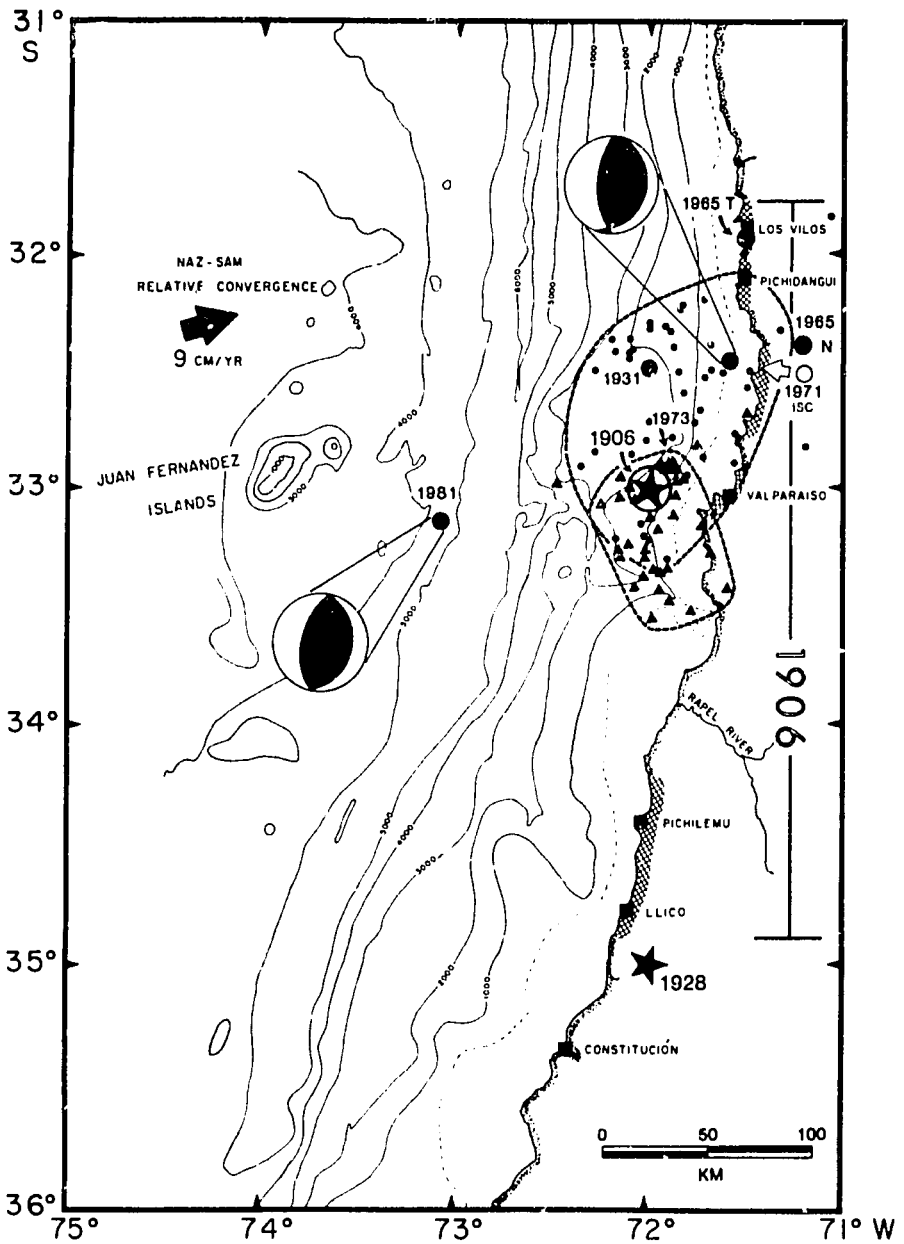

Fig. 8. Recent earthquakes and rupture zones within and near the Valparaiso seismic gap. Coastal outline and bathymetry (contour interval 1000 m) from Prince et al. [1980]. Epicenters from Gutenberg and Richter [1954], Eisenberg et al. [1972], Malgrange et al. [1981] and the Earthquake Data Report of the U.S. Geological Survey (1982). The locations of aftershocks associated with the 1971 (solid small circles) and 1973 (solid small triangles) events are from the ISC Bulletin. Hachured segments of the coast are those areas of observed coastal uplift associated with the 1906 earthquake [Davison, 1936]. These uplift data constrain the rupture length to extend from about 31.7° to 34.9°S. The epicenter of the 1906 event is denoted by an encircled star. Note that both the 1971 and 1973 rupture zones appear to be sharply terminated to the south by a NW trending canyon on the trench inner wall. The 1965, 1971 and 1973 events are all clustered in the northern half of the 1906 rupture zone, near the intersection of the Juan Fernandez Islands with the Chile trench. The southern segment of the 1906 zone (from 33.5° to 35°S) has been quiet for large shocks since 1906, and may be the next segment to rupture. The 1981 event (M_s7.2) occurred on the trench outer rise and is indicative of compressive stresses in a tectonic regime that globally is normally a tensional environment. Focal mechanisms of the 1971 and 1981 events are from Malgrange et al. [1981] and the Earthquake Data Report, respectively.

thickness of trench axis sediments south of 33°S [Schweller et al., 1981]. On land, this intersection is associated with the absence of Quaternary volcanism and the Longitudinal Valley north of 33°S, and a steep gradient in the average elevation of the Andes and the coastal ranges in the vicinity of 33°S [Barazangi and Isacks, 1976; Pilger, 1981; Lowrie and Hey, 1981; Jordan et

al., 1983]. In Figure 8 note that all of the large and great shocks in this area since 1906, with the exception of the 1928 Talca shock, are located in the vicinity of the Juan Fernandez-Chile margin intersection at 33°S.

The August 16, 1906, Valparaiso earthquake (M_w8.2-8.6) ruptured a segment of the Chilean margin from 32° to 35°S [Steffen, 1907; Davison, 1936; Lomnitz, 1970; Kelleher, 1972] based on the extent of observed coastal uplift shown in Figure 8. In the region from Rio Liqua to Quintero (32.4°-32.7°S) the uplift ranges from 27.5 to 31.5 inches (0.7 to 0.8 m), and was no greater than 31.5 inches farther north [Davison, 1936]. Along the bay of Valparaiso, a band of shallow water molluscs (Balanos) and corals were uplifted 2 feet (0.6 m) above low water level. In Figure 8, the location of the epicenter with respect to the rupture zone suggests that the 1906 event was a bilateral rupture.

The first documented observations of coastal uplift along the Chilean margin are associated with the November 19, 1822, Valparaiso earthquake. Graham [1824] estimated the elevation change of the coast at Quintero (32.7°S) to be approximately 4 feet (1.2 m), as evidenced by exposed beds of oysters, mussels and other shellfish. Farther south, at Valparaiso (33°S), the coast is estimated to have been uplifted by about 1 to 6 feet (0.6-1.8 m) [Graham, 1824; Meyen, 1836; Lyell, 1853; Robison and Joy, 1836]. The extent of coastal uplift associated with the 1822 event is poorly known, as both Graham's [1824] and Robison and Joy's [1836] observations are confined to the Quintero-Valparaiso region. In 1835, Darwin [1838] found a barnacle line that was uplifted 3 to 4 feet (0.9-1.2 m) above the tidal level, near the mouth of the Rapel River (33.9°S). Davison [1936] associates this uplift with the 1822 shock.

In Figure 9, estimates of coseismic uplift associated with the 1822 and 1906 shocks are shown for three localities: Quintero, Valparaiso and the Rapel River-Llico region. The shaded bands in Figure 9 represent the average recurrence date (1992±10 years) based on historic repeat times in this zone. The distribution of past uplifts and recurrence times fits either the time-predictable (T.P.) or slip-predictable (S.P.) models reasonably well. Extrapolation of the time-predictable slope (based on the uplift estimates for two previous shocks) indicates a recurrence date in the mid-1960's. Following the notation of Sykes and Quittmeyer [1981], the calculated recurrence time is

$$T_{r_{?-1906}} = \frac{\text{Uplift}_{1906}}{\text{Uplift}_{1822}} T_{r_{1906-1822}}$$

or in this case, 0.75 m/1.10 m x 84 years=57 years or 1963. The error in this date is assumed to be dependent on the observed range of measurements and is estimated to be about ±20-30 years. Extrapolation of the slip-predictable slope (based on three previous events) suggests that events with displacements similar to the 1906 and 1822 earthquakes should occur in the time period 1982-2002. The rate of coseismic crustal uplift at the localities shown in Figure 9 can be estimated from the time- and slip-predictable slopes,

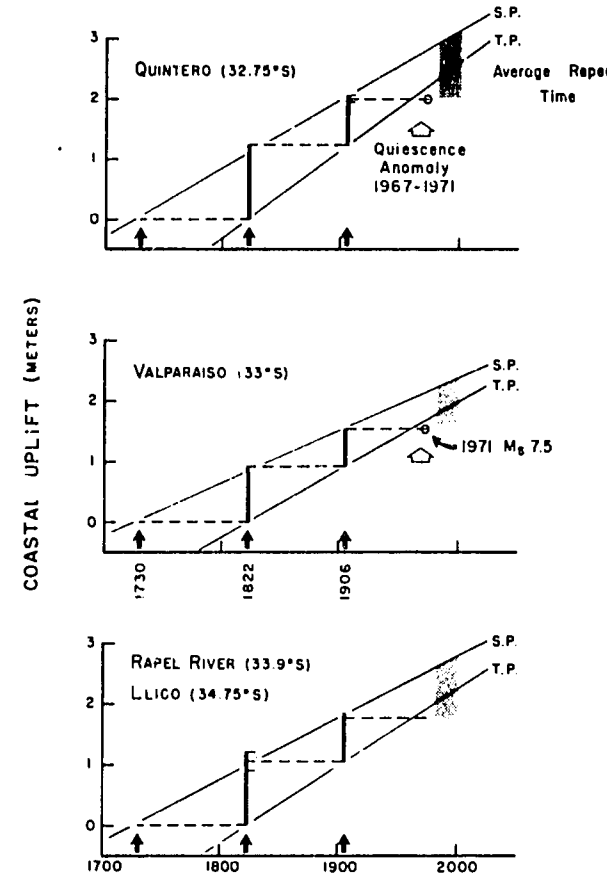

Fig. 9. Coseismic coastal uplift associated with the 1822 and 1906 Valparaiso, Chile, earthquakes and recurrence date estimates. Reports of coseismic coastal uplift from Graham [1824], Robison and Joy [1836], Darwin [1838], Davison [1936] and Lomnitz [1970] for the Quintero, Valparaiso and Rapel River-Llico region. The shaded bands are the average repeat time ±2σ (86±10 years). S.P. and T.P. represent behavior according to the slip- and time-predictable models, respectively. Both the time- and slip-predictable curves fit the data reasonably well. The slip-predictable model suggests that displacements similar to the 1906 and 1822 shocks should occur between 1982 and 2007. The time-predictable model suggests that this region should have reruptured during the mid-1960's. It is significant that during this time interval, a clearly identifiable quiescence anomaly (arrow) preceded the 1971 M_s7.5 Valparaiso earthquake, which ruptured about 1/3 to 1/2 of the 1906 zone.

and ranges from 0.85 to 1.45 cm/yr. For comparison, Darwin [1838] estimated the long-term rate of uplift during the period 1634-1822 to be approximately 2 cm/yr, based on the change in position of a high water mark on the foundation of the church of San Augustin in Valparaiso.

Another estimate of recurrence time is available by dividing the amount of displacement in the preceding earthquake by the rate of convergence. Unfortunately, the seismic moment of the 1906 Valparaiso earthquake is poorly known, partially because of the lack of long-period instrumentation and partially because of the occurrence of a large Aleutian earthquake 30 min before. Various estimates of the magnitude of the 1906

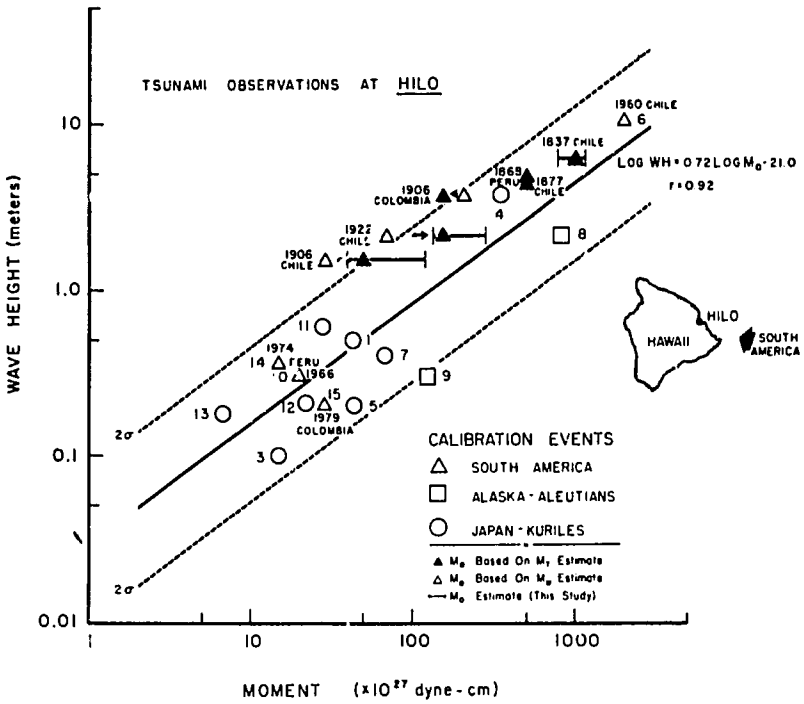

Fig. 10. Tsunami observations at Hilo, Hawaii. Tsunami wave heights, recorded at Hilo, Hawaii, are plotted as a function of seismic moment for a set of calibration events (open symbols). Calibration shocks (i.e., those events with instrumentally determined seismic moments) and M_t estimates are from Abe [1979]. A least squares fit and associated 2σ standard deviation for the calibration data set are shown as solid and dashed lines, respectively. Wave heights for all South American tsunamis plot above the solid line. Note that the M_w estimate for the 1906 Valparaiso shock (M_w8.2, Mo 28 X 10^{27} dyne cm [Kanamori, 1977a]) lies outside of the 2σ confidence limits and appears to be underestimated. The M_t estimate of M_0 (50 X 10^{27} dyne-cm, solid triangle) is in better agreement with the estimates discussed in the text (solid bar) and the general trend of other South American tsunamigenic earthquakes.

shock range from M_s=8.1 to 8.6, M_w=8.2 [Geller and Kanamori, 1977; Kanamori, 1977a; Abe, 1983]. Two independent data sets which can constrain the amount of displacement are the extent of coastal uplift and tsunami wave heights. Figure 10 shows tsunami wave heights recorded at Hilo, Hawaii, as a function of seismic moment. The moment estimate for the 1906 event, as based on the M_w value of 8.2, clearly falls outside the general trend of other South American tsunamis recorded at Hilo. This suggests that the seismic moment has been significantly underestimated. Using a rupture length based on the extent of coastal uplift (about 330 km), and assuming the rupture broke the entire downdip portion of the plate interface (100-150 km), the displacements range from 320 to 620 cm and the calculated moment ranges from 40 to 120 x 10^{27} dyne cm. These values are in better agreement with the trend of South American tsunamis in Figure 10, and are in reasonable agreement with Abe's [1979] M_t estimate (M_t=8.4). The corresponding M_w values based on the above values of M_0 range from 8.5 to 8.7. Using the above displacement estimates (3 to 6 m) divided by the convergence rate (9 cm/yr), the estimated recurrence time ranges from 33 to 67 years, assuming no aseismic slip.

The above estimate of recurrence time for the 1906 shock (33 to 67 years) is shorter than observed in the historic record for an earthquake of this apparent size (86 years). This discrepancy may reflect errors in the estimates of displacement or the presence of aseismic slip in the area. Both assumptions can be tested by plotting the estimates of cumulative coseismic displacement for previous shocks as a function time (see Figure 11). Data for the earlier shocks are summarized in Table 2. As in Figure 9, least squares fits to both the maximum and minimum displacement estimates fit both the time- and slip-predictable models reasonably well, although the slip- predictable fits miss the earlier 1647 shock. For the time-predictable fits to the data, α ranges from 0.57 to 0.85. The validity of the above relationship, of course, depends on the accuracy of the displacement estimates used. Lomnitz [1970] and Kelleher [1972] infer that the rupture area for the November 19, 1822, shock is approximately equal to that of the 1906 shock. The coastal uplift data in Figure 9, however, indicate that the 1822 event may have been even bigger. Hence, the estimate of α based on 3 m of displacement probably represents a lower limit. The July 8, 1730, event is one of the largest shocks to occur in the Valparaiso region. Lomnitz [1970] notes that this event damaged houses on the hillsides of Valparaiso that were largely spared in the 1906 event. Kelleher [1972] infers that this event broke the same segment as the 1906 Valparaiso and 1943 Illapel shocks (zones 5 and 6).

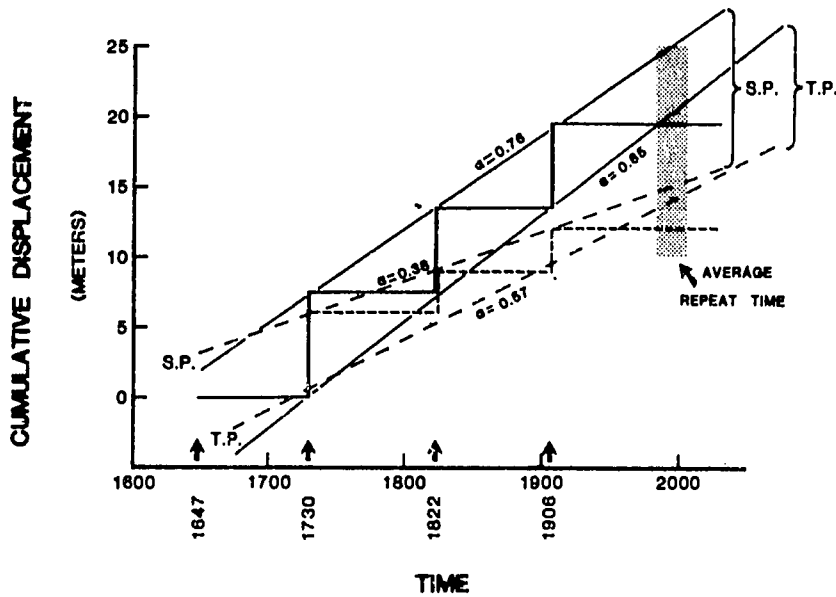

Fig. 11. Cumulative displacement and recurrence estimates for the Valparaiso seismic zone. Solid (and dashed) lines represent the maximum (and minimum) average displacements for prior great shocks in the Valparaiso area as calculated from the data in the text and scaling laws. Shaded band is the extrapolated average repeat time (86±10 years). S.P. and T.P. represent least squares fits to the data according to the slip- and time-predictable models of recurrence, respectively. Both curves fit the data reasonably well, and help constrain both the amount of aseismic slip in the area (15% to 40%) and a recurrence time. The T.P. fit to the minimum estimates (α=0.57) indicates a recurrence in 1955, while the T.P. fit to the maximum estimates indicates a repeat within the next few years. Both of the S.P. fits, while missing the earlier 1647 event, indicate the recurrence of a characteristic or similar-sized shock within the next 20 years, as well.

Using this rupture length (350-450 km) the estimated displacement ranges from 600 to 750 cm. The data in Figure 11 suggest that some amount of aseismic slip is occurring in this region. Using the average displacement of 500 cm for the 1906 shock, the estimated recurrence time ranges from 64 to 92 years for α=0.85 and 0.6, respectively, or 1970-1998. These dates fall within the time- and slip-predictable estimates based on coastal uplift shown in Figure 9.

In summary, the deterministic recurrence time estimates range from 57 to 117 years (see Table 2). For an average recurrence time of 79 years, the conditional probability ranges from 76% to 96% and is somewhat higher than the Weibull estimates of 33% to 75% or the Poisson estimates of 22% (see Figures 2 and 3).

Zone 6: Coquimbo - Los Vilos, 30°-32°S

Previous great shocks that have ruptured this segment of the margin occurred in 1730, 1880 and 1943. This zone lies within the region of the Chilean margin associated with a shallow dipping intermediate depth subduction zone. The end points of the April 6, 1943, Illapel (M_s 7.9, M_t 8.2) event are poorly determined and Kelleher [1972] estimates that the rupture extended from 30.2° to 32.2°S. The area of MM VII damage associated with the August 15, 1880, shock is more than 100 km long and both Lomnitz [1970] and Kelleher [1972] consider this shock to be similar in size to the 1943 event. Little is known about the extent of the July 8, 1730, shock in this area, and it is not known if there were any other large shocks in the time period 1730-1880. In light of the size of the 1943 event (M_t=8.2) the 63-year repeat time between the two previous events (1943-1880) appears to be a reasonable estimate for the recurrence time of the next Illapel shock. The conditional probabilities range from 52% to 66% and are consistently higher than either the Weibull distribution estimates (3% to 6%) or the Poisson estimates (27%). This is not too surprising, as the Weibull distributions are dominated by recurrence times longer than 80 years, and the deterministic estimates are dominated by the fact that the most recent earthquake was not very large and is estimated to have a recurrence time less than 80 years.

Zone 7: Copiapo - Coquimbo, 26°-30°S

While this area has experienced a number of large shocks during the late eighteenth, nineteenth and twentieth centuries, only the March 30, 1796, and November 10, 1922, events appear to be great shocks that ruptured this entire segment [Lomnitz, 1970]. McCann et al. [1978, 1979] noted that the historic record for this section of the Chilean margin was incomplete, and assigned this area to category 3 (historic record incomplete, may have potential for a large earthquake). Zone 7 lies within the megatectonic segment of the Chilean margin characterized by a shallow intermediate depth seismic zone and a lack of Quaternary volcanism [Barazangi and Isacks, 1976], and is similar to

18

the shallow dipping subduction zone in central Peru. Forearc structures along the entire length of the flat zone (27°-33°S) indicate Quaternary stability, as opposed to observations of active uplift and subsidence in the segments above the normally dipping Benioff zone to the north and south [Jordan et al., 1983].

The epicenter of the great 1922 Atacama Desert shock (M_w8.5, M_t8.7) is located about 100 km inland, whereas most great tsunamigenic shocks have epicenters at or near the coast. This was apparently a complicated multiple event, as two great shocks were felt within the first 8 min and many large "aftershocks" followed immediately [Lomnitz, 1970]. The actual rupture dimension is poorly known and ranges from about 300 to 450 km based on the extent of coastal uplift, damage reports and S-P data [Kelleher, 1972]. Using the above dimensions, the M_o estimated for this event ranges from 130 to 300 x 10^{27} dyne cm (see Table 2) and falls within the trend of other South American tsunamis (Figure 10).

Lomnitz [1970] states that the 1796 shock may have been similar to the 1922 event; however, no tsunami was generated by the former. Large events in 1849 and 1859 are poorly documented. Hence, there are few data to constrain either α or the time- and slip-predictable models. Assuming that 1922 style events are typical for this region and 600 to 1100 cm is a reliable estimate of the displacement, the corresponding repeat times range from 74 to 135 years (α=0.90-1.00), for an average of 104 years. Using the 1796 shock as the previous event (T=126 years), T/T_{exp}=1.21. The 104-year estimate for the recurrence of the 1922 shock gives conditional probabilities in the 21% to 24% range, which are slightly higher but in general agreement with the Weibull (4% to 18%) and Poisson (17%) estimates for this zone.

Zone 8: Taltal - Coquimbo, 25°-27°S

As well as being involved in the infrequent great shocks which occur in this region, this area has also produced a number of large shocks during the last two centuries. This zone lies within the rather diffuse tectonic boundary between "normal" subduction to the north and "shallow" subduction to the south (zones 6 and 7). Within the trench, this boundary may be associated with an abrupt jump in trench axis depths at about 27°S [Schweller et al., 1981]. On land, Jordan et al. [1983] also place this boundary at about 27°S, based on the continuity of forearc and magmaticarc features. Previous large events during this century have occurred in 1918, 1939, 1946, 1965-1966, 1978 and 1983. The estimated average displacements for the 1966 Taltal and 1978 Copiapo shocks are 200 and 70 cm respectively, and at 9 cm/yr, the estimated recurrence times range from 22 to 8 years. For a 20 year-time window, the estimated conditional probabilities are all at the 99% to 100% level. For comparison, the Weibull estimates based on data from this and zone 3A are 45% to 58% and the Poisson estimates are at the 46% to 60% level. It is of interest to note that a M_s 7.3 shock occurred in the vicinity of the 1978 event on October 4, 1983. The apparent repeat time is about 5 years and is within the time frame of the estimates presented above. The occurrence of this shock, however, when viewed in a 20-year time span does not significantly reduce the hazard for this area, as the estimated recurrence times are shorter than 20 years (see Figure 6).

Zones 9 and 10: Mollendo - Arica - Antofagasta, 17°-24°S

Of the 10 seismic zones considered in this study, both zones 9 and 10 stand out as having the longest elapsed time since a prior great shock [McCann et al., 1978, 1979]. The great (M_t 9.0) earthquake of May 9, 1877, ruptured the northern segment of the Chilean margin from about 18° to 25°S and produced a destructive Pacific-wide tsunami comparable in size to those produced by the 1960 and 1837 shocks in zone 3 (see Figure 10). South of Antofagasta (23.5°S) there are no felt or tsunami reports associated with the 1877 shock until Caldera (27°S) [Milne, 1880]. The segment of the Chilean margin between Antofagasta and Caldera is also coincident with a region of no known large or great earthquakes during this century (segment with a question mark in Figures 2 and 3). The 1877 shock may have also ruptured this segment of the margin as well as the more populated segment to the north of Antofagasta, for a total rupture length of 650 km. It is not clear whether the 1877 earthquake is the only historic event for the zone 9. Arica (18°S) was destroyed by a great tsunamigenic shock on November 24, 1604, and except for the 1868 event, discussed below, there are no reports of great tsunamigenic shocks in the intervening time. Since the seismic history for this region is incomplete, deterministic estimates similar to others discussed in this study cannot be made at present. Based on the available data we can roughly estimate a recurrence time. Both the 1868 and 1877 earthquakes were assigned M_t magnitudes of 9.0 [Abe, 1979], which corresponds to a seismic moment of about 350-400 x 10^{27} dyne cm. For the 1877 event, Lomnitz [1970] estimates the zone of highest intensity to extend along the coastline for approximately 450 km. Taking a slightly larger dimension (550 km) and using the above M_o estimate and scaling laws, the estimated displacement in 1877 is 800-1200 cm. Dividing this estimate by the convergence rate (9 cm/yr), assuming no aseismic slip, results in a repeat time of 88 to 133 years (i.e., 1966-2010). For an average repeat time of 111 years, the conditional probability ranges from 59% to 85% and is significantly higher than the probabilities under the Poisson assumption (16%). Hence, the potential estimates based on the criteria of McCann et al. [1978, 1979] and the extrapolation of the Weibull estimates (Figure 2) could well be accurate representations of the level of seismic hazard in this area. Of course, increasing the amount of aseismic slip in this region would proportionally increase the repeat time and decrease the level of seismic potential.

While there are no direct estimates of aseismic slip for this region, we can make use of tectonic similarities along strike of the Chilean margin and around the circum-Pacific to provide a somewhat crude, but important estimate of this parameter. Wortel and Vlaar [1978], Wortel

19

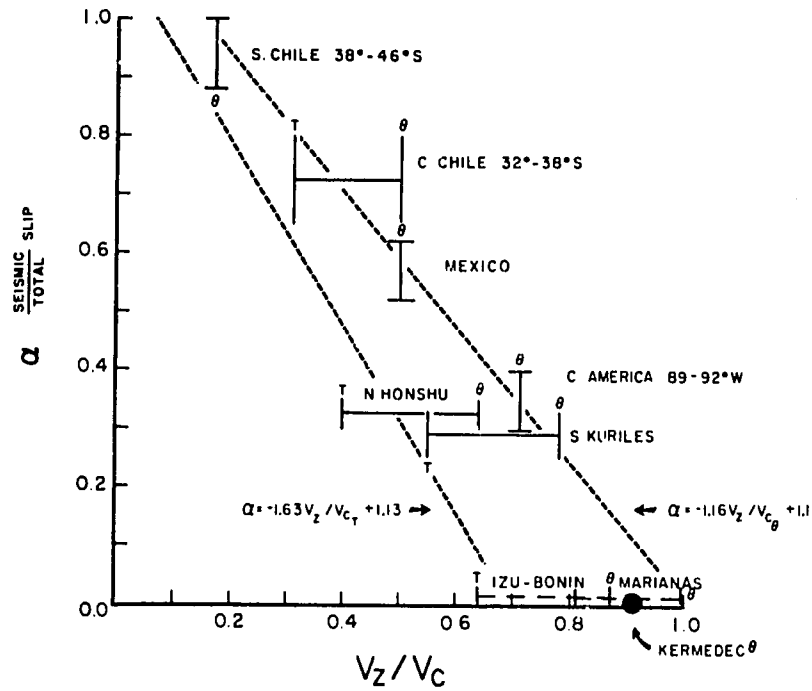

Fig. 12. Global variation of the ratio of seismic/total slip as a function of the trajectory of the subducted oceanic lithosphere. Values of α (seismic/total slip) based on studies of large and great earthquakes by Kanamori [1977b], Sykes and Quittmeyer [1981] and this study. Values of α are dashed where inferred (i.e., no history of great earthquakes). Values of V_z/V_c are based on the dip of the intermediate depth seismic zone (θ estimates) and depth/reabsorption time calculations by Wortel [1980] (T estimates). Dashed lines are the least squares fits to the T and θ estimates. While scattered, the data suggest at least a first-order relationship between the partitioning of convergence into seismic and aseismic slip and the geometry of the subducted slab. Wide interfaces and shallow dipping slabs have less aseismic slip than narrow interfaces and steeply dipping slabs.

[1980] and England and Wortel [1980] emphasize the role of lithospheric age and penetration depth of subducted oceanic crust in determining the tectonic evolution of the South American margin. These concepts are further developed by Ruff and Kanamori [1980], who found strong correlations between convergence rate, lithospheric age and the size of great earthquakes on a global scale. Qualitatively, it is suggested that trajectory of the subducted slab (determined by the horizontal convergence rate and the vertical sinking velocity) influences the degree of mechanical, and presumably seismic coupling, between two interacting plates at a subduction zone. Underthrust oceanic crust that had a shallow trajectory would have more mechanical coupling than underthrust crust with a steeper trajectory. Hence, it may be possible to infer the regional distribution of seismic slip based on readily observed parameters such as age, depth and dip angle of the subducted oceanic lithosphere.

For a few segments of the circum-Pacific convergence zone, the amount of aseismic slip has been determined using the data set of large and great earthquakes and their repeat times [Kanamori, 1977b; Sykes and Quittmeyer, 1981]. The slip during these events accounts for the majority of convergent plate motion and presumably is a reasonable estimate of the long-term partitioning of convergence into seismic and aseismic slip. In Figure 12, estimates of α (ratio of seismic/total slip) are plotted as a function of the ratio of vertical to horizontal plate velocity (V_z/V_c). The convergence rate V_c is based on the pole of rotation from Minster and Jordan [1978], and the vertical velocities V_z are calculated via (1) $V_z=V_c \sin \theta$, where θ is the dip of the intermediate depth seismic zone (values of θ from Uyeda and Kanamori [1979]) and (2) maximum depth/reabsorption time calculations by Wortel [1980]. Along many convergent margins, the values of θ are poorly known for the shallow portion of the subduction zone. It is possible, however, to correlate aseismic slip and slab trajectory using the more readily available parameters for intermediate depth seismic zones as is shown in Figure 12.

Using Figure 12 as a guideline, we can now estimate the amount of aseismic slip in northern Chile and southern Peru. This segment of the South American margin, from 15° to 25°S, is characterized by a deep, continuous seismic zone (300 km) with a relatively steep dip (30°) [Barazangi and Isacks, 1976]. The age of the seafloor at the trench is anomaly 18-20 age (41-44 m.y. B.P.), and is one of the oldest segments of the Nazca plate presently being subducted. In northern Chile, the ratio of vertical to horizontal velocity is estimated to be greater than in central or southern Chile (0.5 versus 0.4-0.2), and α is estimated to range between 0.3 and 0.6. In other words, based on the global comparison in Figure 12, between 40% and 70%

20

aseismic slip is estimated to be occurring in northern Chile. Using these estimates of α, and our estimate of displacement during the 1877 shock, the repeat time ranges from 148 to 444 years or 2025 to 2321. Using an average repeat time of 296 years, the resulting conditional probabilities range from 0.07% to 1.4%. Of course, these are only estimates based on a limited data set; however, the values they describe are consistent with the overall framework of subduction along the Chilean margin and the historic record.

The M_t value of 9.0 assigned by Abe [1979] to the 1868 Arica shock is similar to that of the 1877 event; however, the great circle paths to Hilo and other tide gauge stations sample different portions of the tsunami radiation pattern for both events. Great circle paths from Antofagasta to Hilo are approximately normal to the trench, while the paths from Mollendo to Hilo are approximately parallel to the Peru-Chile trench. The largest far-field waves associated with tsunamis are found within about $\pm 30^{\circ}$ from the perpendicular to the fault [Ward, 1981]. The wave heights seen at Hilo for the 1868 event were presumably generated near a node in the tsunami radiation pattern, and the M_t value of 9.0 may be a lower bound for the size of this earthquake. Using the same displacement and repeat time estimates determined for the 1877 shock, the conditional probabilities range from 65% to 91% with no aseismic slip and 0.13% to 1.8% with about 50% aseismic slip, for the next 20 years. Given that the only historic repeat for a great tsunamigenic shock in this region is 264 years, the above estimates based on aseismic slip do not appear too extreme.

In summary, the seismic potential for the Big Bend region of northern Chile and southern Peru (zones 9 and 10) is still poorly known, as seen in the wide variation of probability estimates (<1% to 91%). When great earthquakes occur in this region, they potentially could be as large as the 1868 and 1877 series of shocks. Hence, both areas should be regarded as having an unconstrained but significant amount of seismic potential.

Discussion

This paper attempts to quantitatively assess the seismic potential or probability of recurrence during a specified period of time for various segments along the convergent margins of Chile and Peru by applying statistical and deterministic techniques. The concept of seismic potential is presented in both a stochastic and deterministic or semistochastic framework via the use of Weibull distributions and the time-predictable model of earthquake recurrence. The estimates of seismic potential presented in this study are meant to be interpreted as long-term forecasts only, as the resolution capability (or standard deviation) of these techniques is ±15% to ±25% of the repeat time. While the absolute levels of probability may be uncertain by a factor of 2, both historic and deterministic techniques can be used to place constraints on the relative level of seismic potential with respect to other segments of the Chilean margin. The estimates of potential presented in this paper allow for a more detailed evaluation of earthquake hazard than was available for McCann et al. [1978, 1979]. A better estimation of seismic potential, in turn, can allow for a clearer understanding of the significance of seismicity processes and possible precursory phenomena.

Much of the analysis done in this paper relies on scaling laws [Sykes and Quittmeyer, 1981; Scholz, 1982] for estimates of displacement and seismic moment. An important assumption for all of these results is that displacement is uniformly distributed over the entire fault surface. For many events with fairly constant rupture dimensions and repeat times, this assumption appears valid. There are also many cases, however, where the amount of displacement varies significantly along strike (e.g., the 1857 Fort Tejon earthquake in southern California [Sieh, 1978], and the 1906 San Francisco earthquake in northern California [Lawson, 1908]). Sykes and Nishenko [1984] show that these variations in displacement can have a direct bearing on the recurrence history and hence estimates of potential. Areas with less displacement are likely to have earlier repeats than segments with larger amounts of displacement. Estimates of seismic potential which do not take into account these variations could be in error by a factor of 2 in repeat time for various segments of the same rupture zone.

The temporal resolution or inherent error in the deterministic recurrence estimates can be evaluated using the ratio T/T_{exp} (where T is the actual repeat time and T_{exp} is the estimated repeat time) and the recurrence time estimates for prior shocks discussed throughout the text. For convenience, the ratio T/T_{exp} is assumed to be normally distributed around a mean value (see Appendix B). In Figure 4, the histogram shows the distribution of T/T_{exp} and the resulting fit (mean=0.90 and σ=0.15, σ is the fraction of the repeat time, and the actual standard deviation in years is σT_{exp}). Comparing the two distributions in Figure 4, it is clearly apparent that the degree of resolution is similar for both methods. The distribution in Figure 4b also shows a tendency for recurrence estimates to be slightly overestimated by about 10% of the actual repeat time. Whether this 10% overestimation reflects a systematic error in the calculation of T_{exp} or a bias from a limited sample population is not clear. The effect of the 10% shift in the position of the mean is to increase the probability estimates by as much as 20% for any given value of T/T_{exp}. Overall, the lack of resolution, to less than ±15-25% of the repeat time reflects the quality of data available from historic accounts of great earthquakes and the inherent errors in the estimation of earthquake source parameters using scaling laws, convergence rates, amounts of aseismic slip, etc. This level of resolution (±15%) is similar to that found by Sykes and Quittmeyer [1981] using the time- predictable model and a global survey of three or more recent earthquakes. Only in those cases where rupture dimensions vary by a factor of 1.5 or greater can the time- or slip-predictable models be distinguished based on the available data. I have assumed the time-predictable model as a working

21

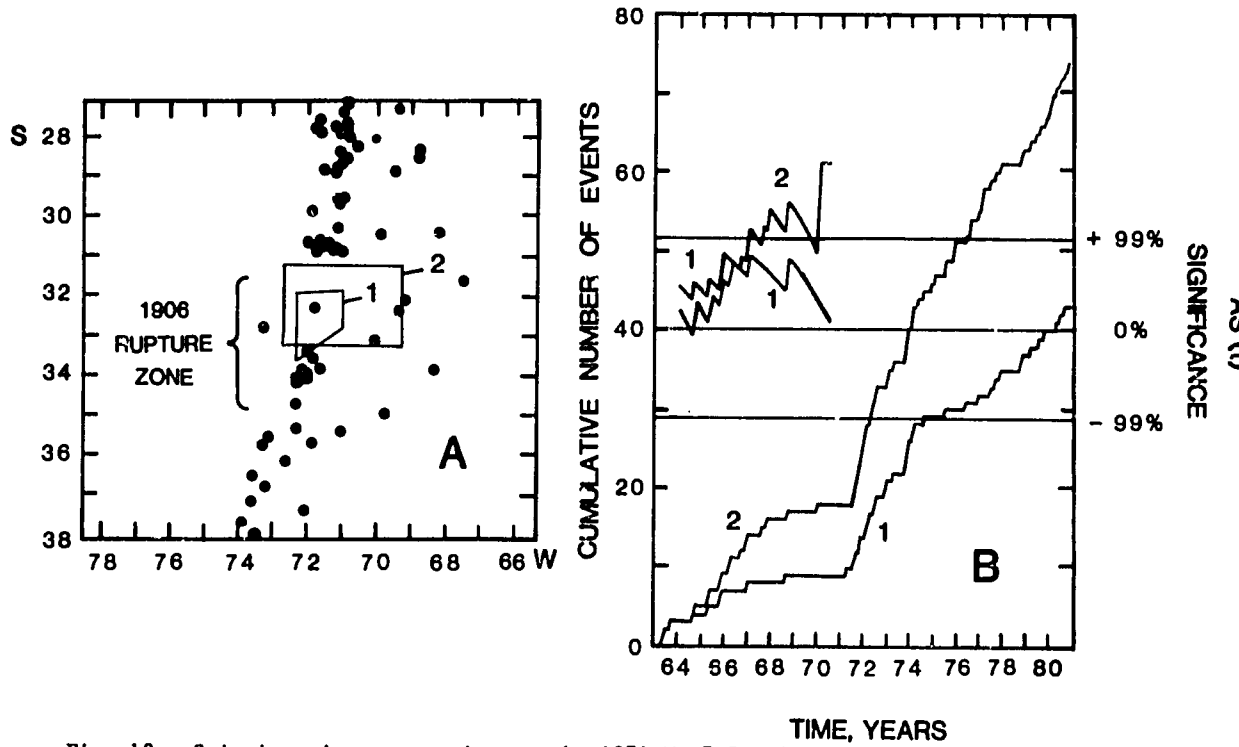

Fig. 13. Seismic quiescence prior to the 1971 M_s 7.5 Valparaiso earthquake, from Habermann [1979]. (a) Map showing events with $m_b \geq 4.7$ for a segment of the Chilean margin (27°-38°S) from November 1967 to July 1971. These dates define the period of quiescence prior to the 1971 shock. The 1971 shock ruptured the smaller polygon (labelled 1); the zone of seismic quiescence (larger rectangle, labelled 2) includes 1/2 of the 1906 rupture zone. (b) Cumulative number of independent events (aftershocks and clusters removed) with $m_b \geq 4.7$ occurring in the rupture zone of the 1971 event (curve 1) and the larger rectangle (curve 2). Also shown is the AS(t) function [Habermann, 1981] for the period November 1967 to July 1971 for both regions. The scale for the AS(t) function is indicated on the right hand side of the graph. The upper and lower boundaries indicate rate decreases (increases) that are significant at the 99+% level. For the 1971 event, the quiescence anomaly is significant at the 99% level in the larger rectangle, but is not as significant within the actual rupture zone itself.

hypothesis for the majority of calculations presented in this paper. For the majority of historic events, it appears that the models of earthquake recurrence are capable of finer resolution than the data at present can provide.

A comparison between the historic, deterministic and Poisson estimates of conditional probability (or seismic potential) for the next 20 years (1984-2004), as listed in Table 1 and discussed in the text, is summarized in Figures 2 and 3. For three of the 10 zones considered (zones 3, 3A and 8) there is a basic agreement between the probabilities calculated via these three methods. All three zones are characterized by either high (50-100%) or low (0-20%) probabilities. For the Poisson estimates, which are independent of the amount of time elapsed, this agreement reflects the fact that either the previous shock occurred a short time ago and the estimated recurrence time is very long (zone 3) or that the repeat times are shorter than the 20-year time span used for the conditional probability calculation (zones 3A and 8). For the remaining seven zones, the Poisson estimates tend to systematically underestimate the level of conditional probability and hence offer little in the way of providing a basis for long-term earthquake forecasting. Both the Valparaiso (zone 5) and Big Bend (zones 9 and 10) regions have high probabilities for recurrence according to the historic and deterministic estimates and are considered likely sites for large or great shocks before or near the turn of the century. For zones 9 and 10, however, the high probability estimates are poorly constrained. Comparison with historic repeat time behavior in central and southern Chile suggests probabilities at the 30% to 100% level, while deterministic estimates indicate probabilities at the 1% to 90% level. Clearly, in view of the possible high seismic hazard in this area, more work needs to be done to document the recurrence history and constrain the level of potential. The discrepancy in potential estimates for the Illapel (zone 6) and Concepcion (zone 4) regions apparently lies in the fact that the historic record for great shocks along this section of the Chilean margin is dominated by recurrence times greater than 80 years, and the previous shocks in both of these regions are estimated to have recurrence times less than 80 years. In fact, the 1928 Talca zone should have already reruptured according to the time-predictable estimates presented (see Table 2). This is a small zone, however, and strain

22

release may be dependent on the behavior of the adjoining segments. Nevertheless, the large contrast in the hazards estimates pinpoints this area for more detailed investigations to resolve this conflict.

In Figures 2 and 3 note the spatial proximity of areas with high deterministic levels of probability (zones 4, 5 and 6 and zones 9 and 10). Studies of time-dependent rupture [Das and Scholz, 1981] and models of viscoelastic coupling [Lehner and Li, 1981] suggest that a large or great shock on one fault segment may trigger activity on an adjacent segment (provided the adjacent segment is close to failure) and produce a larger event than either segment could alone. Both Figures 2 and 3 indicate that a 1000-km segment of the margin (including zones 3A, 4, 5 and 6) has a relatively high probability for a series of large or great earthquakes during the next 20 years. This type of behavior, where adjacent segments of the margin rupture within a short amount of time, does not appear different from previous recurrence cycles where zones 3, 4 and 5 have all ruptured within a 20- to 30-year time span [see Kelleher, 1972, Figure 2].

The high level of seismic potential for the Valparaiso gap during the next 20 years (33-75% via Weibull distributions; 70-92% via deterministic models) is fairly well constrained and is in good agreement with the more qualitative observations by Kelleher [1972] and McCann et al. [1978, 1979]. In view of the 35-year uncertainty in recurrence time estimates (1963-98) for the Valparaiso gap, the seismic activity in this region during the last 20 years is of considerable interest and is summarized in Figure 8.

The July 9, 1971, Valparaiso earthquake (32.5°S, 71.2°W, M_s=7.5, M_0=5.6 x 10^{27} dyne cm, Malgrange et al. [1981]) ruptured a segment of the coast extending from 32° to 33.2°S. The rupture zone, as defined by aftershocks occurring during the first 5 days after the July 9 main shock, is shown in Figure 8, and covers about 1/3 of the 1906 zone. In 1973, a M_s6.7 shock occurred at the southern end of the 1971 rupture zone and overlapped that zone (Figure 8). Both aftershock zones appear to be sharply terminated to the south by a northwest trending submarine canyon on the trench inner wall. This canyon is located slightly south of the major onland transition between the N-S trending Longitudinal Valley and the E-W trending Transverse Valley at 33°S, and may represent a boundary between two crustal blocks. Farther south, near 34°S, the Chilean trench changes strike from N-S to NE-SW near the location of a second major submarine canyon. The onshore continuation of this canyon is near 35°S, the southern limit of the 1906 shock and the epicenter of the 1928 Talca earthquake.

For the time period before the 1971 event, Habermann [1979] noted a zone of seismic quiescence for moderate-sized earthquakes that extended from 31.2° to 33.2°S, covering an area larger than the eventual 1971 rupture zone and approximately 1/2 of the 1906 zone. This zone was quiescent for all events of $m_b \geq 4.7$ between November 1967 and July 1971 at the 99+% significance level (Figure 13). The 42-month period of seismic quiescence is interpreted as a precursor to the 1971 event, and is similar to the precursory quiescence prior to the 1978 Oaxaca, Mexico, earthquake [Ohtake et al., 1977]. The episode of seismic activity (and inactivity) that began in 1965 coincides with the time-predictable estimate of recurrence (1963) based on coseismic coastal uplift in Figure 9. This correlation may be a coincidence or it may indicate that this region had recovered most of the strain released in 1906 and was in the preparatory stages for another recurrence. The recognition of a clearly identifiable precursor prior to the 1971 Valparaiso earthquake suggests that future large shocks in this region may also be preceded by seismic quiescence for moderate-sized shocks. These shorter-term observations, in conjunction with the long-term forecast presented here, may allow the successful prediction of the next large or great Valparaiso earthquake.

The occurrence of a large (M_s7.2) thrust event at the trench outer rise on October 16, 1981 (see Figure 8), is significant in light of the recurrence estimates for this region. Whereas the majority of shallow outer rise events are tensional in nature and are due to plate bending forces [Chapple and Forsyth, 1979], the rare occurrence of a thrust event in this environment, as Christensen and Ruff [1983] point out, may be symptomatic of the entire region being under E/W compression in preparation for another great interplate earthquake.

In view of the approximate 35-year uncertainty of this analysis, several scenarios can be envisaged for the detailed or short-term behavior of the Valparaiso region [Nishenko, 1982]:

1. The rupture process continues migrating to the south of the 1971 zone, filling in the rest of the 1906 gap. The area from about 33.5° to 35°S would be considered overdue for an earthquake, based on the time-predictable extrapolation of cumulative coseismic uplift shown in Figure 9. This type of behavior may be analogous to that observed in the Colombia-Ecuador seismic zone, where the rupture zone of a great (M_w=8.8) shock in 1906 was subsequently reruptured in a series of smaller shocks in 1941, 1958 and 1979 [Kanamori and McNally, 1982; Mendoza and Dewey, 1984].
2. The 1971, 1973 and 1981 events are "foreshocks" prior to an impending 1906-type event which should occur within the next 25 years and fill in the entire segment from 32° to 35°S. This type of behavior is suggested by the historic record and the slip-predictable interpretation of the uplift and displacement data in Figures 9 and 11.
3. The segment from 32° to 33.5°S reaccumulates the displacement released by the 1971 shock (about 250 cm) within the next 25 to 35 years and reruptures, triggering the adjacent segment to the south (33.5° to 35°S). This scenario is similar in timing to scenario 2, but would behave according to the time-predictable model.

Appendix A: Weibull Distributions

Let the conditional probability of a large or great earthquake occurring at time T in the time interval t and t+Δt be λ(t)Δt, where λ(t) is the hazard function or rate of expected failure at time t, conditional upon survival to time t

23

and $\lambda(t)$ is defined as $f(t)/1-F(t)$, where $f(t)$ is the probability density function and $F(t)$ is the cumulative probability. In probability notation:

$$f(t) = \lim_{\Delta t \to 0} P\,(t \leq T < t+\Delta t)/\Delta t \qquad (A1)$$

$$F(t) = P(T \leq t) \qquad (A2)$$

$$\lambda(t) = f(t)/1-F(t) \qquad (A3)$$

$$\lambda(t) = \lim_{\Delta t \to 0} P\,(t \leq T < t+\Delta t \mid T \geq t)/\Delta t \qquad (A4)$$

The Weibull model assumes the hazard function to be a power function of t:

$$\lambda(t) = Kt^m \qquad (A5)$$

where $k>0$ and $m>-1$. The parameter $\beta=m+1$ describes the shape of the density function. For $\beta=1$, the hazard rate is constant and is the exponential distribution. As β increases, $f(t)$ becomes narrower about the mean recurrence time and the hazard rate increases more rapidly with time. Between $\beta=2$ and 6, the Weibull distribution can be approximated by the normal or Gaussian distribution. The cumulative probability of an earthquake occurring at time t is $F(t)$ where $F(t)=1-R(t)$, and $R(t)$ is known as the reliability

$$R(t) = \exp\left[-\int_0^t \lambda(t)dt\right] \qquad (A6)$$

$$R(t) = \exp\left[\frac{-Kt^{m+1}}{m+1}\right] \qquad (A7)$$

The probability density function or failure density $f(t) = -dR/dt$ or

$$f(t) = Kt^m \exp\left[\frac{-Kt^{m+1}}{m+1}\right] \qquad (A8)$$

The conditional probability function, which represents the probability that an event occurs in a time span τ, provided no event occurs prior to time t is $F_s(t,\tau)$ and is written as $F_s(t,\tau)=F(t+\tau)-F(t)/1-F(t)$ or as $F_s(t,\tau)=1-(R(t+\tau)/R(t))$, where R is the reliability and F is the cumulative probability. For small time increments $\tau \lll T$, the conditional probability asymptotically approaches the hazard rate $\lambda(t)$.

In practice, K and m values for the probability density function are calculated by using the observed failure time or repeat time data to estimate an empirical cumulative distribution $F(t)$. Let n_i be the frequency of repeat times for each time increment chosen. The probability of recurrence within that interval is taken to be $(n_i-1/2)/N$ or $(n_i-3/8)/(N+1/4)$, where N is the sample size. The above plotting rules or rank distributions are superior to the n_i/N or $n_i/(N+1)$ rules since it is unreasonable to assume, based on a small sample of observed repeat times, that 100% of the population would fail prior to the largest observed repeat time. In addition, the two rules used also minimize the bias in estimating the shape parameter β for the Weibull distribution [Mann et al., 1974; Kapur and Lamberson, 1977].

Taking the double natural logarithm of 1/R in equation (A7), the K and m values can be easily determined by the methods of least squares and maximum likelihood, where

$$\ln \ln \frac{1}{R} = \ln\left[\frac{K}{m+1}\right] + (m+1)\ln t \qquad (A9)$$

A goodness-of-fit test applicable to the two-parameter Weibull model is discussed by Mann et al. [1974] and is summarized here. The null hypothesis to be tested is that the population in question is two-parameter Weibull distributed. If the hypothesis is rejected, then another distribution (e.g., the three-parameter Weibull, with a minimum life estimate) should be considered. The test statistic S is

$$S = \frac{\sum_{i=(r/2)+1}^{r-1} \frac{X_{i+1}-X_i}{M_i}}{\sum_{i=1}^{r-1} \frac{X_{i+1}-X_i}{M_i}} \qquad (A10)$$

Let $t_1, t_2, \ldots t_r$ represent the first r ordered failure times for n repeat times in the catalog. Truncate the test at the time of the rth failure ($r \leq n$) and let $x_i = \ln t_i$ for $i=1,2,\ldots,r$. The term r/2 denotes the greatest integer value $\leq r/2$. Values for M_i and the critical values for S can be found in tables by Mann et al. [1974] and Kapur and Lamberson [1977].

Once the m values are calculated from the least squares fits to the data, the mean time interval between t=0 and the next shock (i.e., the mean failure time) can be computed from

$$E(t) = \int_0^\infty t f(t)dt = \left[\frac{K}{m+1}\right]^{-1/m+1} \Gamma\left[\frac{m+2}{m+1}\right] \qquad (A11)$$

where Γ is the gamma function. The mean-square time to rupture is given as

$$E(t^2) = \int_0^\infty t^2 f(t)dt = \left[\frac{K}{m+1}\right]^{-2/m+1} \Gamma\left[\frac{m+3}{m+1}\right] \qquad (A12)$$

The standard deviation of rupture time then is

$$\sigma = \sqrt{E(t^2)-E^2(t)} \qquad (A13)$$

Appendix B: Gaussian or Normal Distributions

The hazard function $\lambda(t)$ specifies the instantaneous rate of failure at time t, conditional upon survival to time t and is defined as in Appendix A,

$$\lambda(t) = \frac{f(t)}{1-F(t)} \qquad (B1)$$

where $f(t)$ is the probability density function for a normal distribution,

$$f(t) = \frac{1}{\sigma(2\pi)^{1/2}} \exp - \frac{(T/T_{exp}-\mu)^2}{2\sigma^2} \qquad (B2)$$

where T/T_{exp} is the fraction of estimated repeat time already elapsed, μ is the mean value of T/T_{exp} (in the case of Figure 4b, $\mu=0.90$) and σ is the standard deviation (0.15-0.25) (see Figure 4b). $F(t)$ is the cumulative distribution function and is written as

$$F(t) = \int_0^t f(t)dt \qquad (B3)$$

As in Appendix A, the reliability R(t) is equal to 1-F(t) and the conditional probability is defined in the same manner.

Appendix C: Poisson Distributions

The basic assumptions governing Poisson or exponential behavior are as follows (1) the occurrence of an event during a time interval Δt is independent of the occurrence of an event prior to the beginning of Δt and (2) the probability of such an event in a time interval Δt is proportional to Δt with a proportionality constant λ, where λ is termed the failure rate. The probability $P_{(r)}$ of failure prior to time t is written as

$$P_{(r)} = \frac{(\lambda t)^r e^{-\lambda t}}{r!} \quad r=0,1,2..... \qquad (C1)$$

and the probability density function is written as

$$f(t) = \lambda e^{-\lambda t} \qquad (C2)$$

The conditional probability for failure in a time interval $t+\Delta t$, given that no failure occurs prior to time t, is

$$P[T>t+\Delta t|T>t] = 1 - \left(\frac{e^{-(t+\Delta t)\lambda}}{e^{-t\lambda}}\right) \qquad (C3)$$

$$P = 1 - e^{-\Delta t\lambda} \qquad (C4)$$

and the conditional probability is independent of t, in this case, the length of time since the previous earthquake, and is only a function of λ and Δt.

Acknowledgements. I thank my advisor, L. R. Sykes, for his support and guidance during this investigation. Discussions with J. Dewey, R. E. Habermann, A. L. Kafka, R. Madariaga, W. R. McCann, D. Perkins, C. Scholz, W. Spence and S. Wesnousky were stimulating and useful throughout the course of this study. Special thanks to my wife, Paloma, for translating, drafting and moral support. L. R. Sykes, P. G. Richards and W. Pitman III reviewed the manuscript. This study was funded by U.S. Geological Survey contract USGS- 14-08-0001-19750, National Science Foundation grant EAR82-12266 and Agency for International Development agreement BOF-0000-P-IC-4051-00. Lamont-Doherty Geological Observatory contribution 3689.

References

Abe, K., Size of great earthquakes of 1837-1974 inferred from tsunami data, J. Geophys. Res., 84, 1561-1568, 1979.

Abe, K., Magnitudes of large shallow earthquakes from 1904 to 1980, Phys. Earth Planet. Inter., 27, 72-92, 1981.

Abe, K., Revised magnitudes of large shallow earthquakes, 1897-1912, Phys. Earth Planet. Inter., 33, 1-11, 1983.

Aki, K., Characterization of barriers on an earthquake fault, J. Geophys. Res., 84, 6140-6148, 1979.

Algermissen, S. T., and D. M. Perkins, A probabilistic estimate of maximum acceleration in rock in the contiguous United States, U.S. Geol. Surv. Open File Rep. 76-416, 46 pp., 1976.

Barazangi, M., and B. L. Isacks, Spatial distribution of earthquakes and subduction of the Nazca plate beneath South America, Geology, 4, 686-692, 1976.

Bobillier, C., Observaciones de 1928 Santiago, Boletin del servicio sismologico de Chile, 1930.

Bufe, C. G., P. W. Harsh, and A. O. Burford, Steady state seismic slip-A precise recurrence model, Geophys. Res. Lett., 4, 91-94, 1977.

Brillinger, D. R., Seismic risk analysis: Some statistical aspects, Earthquake Predict. Res., 1, 183-195, 1982.

Caldcleugh, A., An account of the great earthquake experienced in Chile on the 20th of February 1835, Philos. Trans. R. Soc., London, 126, 21-26, 1836.

Chapple, W. M., and D. W. Forsyth, Earthquakes and bending of plates at trenches, J. Geophys. Res., 84, 6729-6749, 1979.

Christensen, D. H., and L. J. Ruff, Outer-rise earthquakes and seismic coupling, Geophys. Res. Lett., 10, 697-700, 1983.

Cornell, C. A., Engineering seismic risk analysis, Bull. Seismol. Soc. America, 58, 1583-1606, 1968.

Darwin, C., Geological Observations on Coral Reefs, Volcanic Islands and on South America: Being the Geology of the Voyage of the Beagle, Under the Command of Captain FitzRoy, R.N., During the Years 1832 to 1836, 768 pp., London, 1851.

Das, S., and C. H. Scholz, Theory of time-dependent rupture in the earth, J. Geophys. Res., 86, 6039-6051, 1981.

Davison, C., Great Earthquakes, 286 pp., T. Murby, London, 1936.

Eisenberg, A., R. Husid, and J. E. Luco, A preliminary report on the July 8, 1971 Chilean earthquake, Bull. Seismol. Soc. Am., 62, 423-430, 1972.

England, P., and R. Wortel, Some consequences of the subduction of young slabs, Earth Planet. Sci. Lett., 47, 403-415, 1980.

Ewing, M., R. Houtz, and J. Ewing, South Pacific sediment distribution, J. Geophys. Res., 74, 2477-2493, 1969.

Fedotov, S. A., Regularities of the distribution of strong earthquakes in Kamchatka, the Kuril Islands and northeast Japan, Tr. Inst. Fiz. Zemli Akad. Nauk SSSR, 36, 66-93, 1965.

Forsyth, D. W., Fault plane solutions and tectonics of the South Atlantic and Scotia Sea, J. Geophys. Res., 80, 1429-1443, 1975.

Geller, R. J., and H. Kanamori, Magnitudes of great shallow earthquakes from 1904 to 1952, Bull. Seismol. Soc. Am., 67, 587-598, 1977.

Graham, M., An account of some effects of the late earthquakes in Chile, Trans. Geol. Soc., London, 2nd Ser., 1, 413-415, 1824.

Gutenberg, B., and C. Richter, Seismicity of the Earth and Associated Phenomena, 2nd ed., 310 pp., Princeton University Press, Princeton, N. J., 1954.

Habermann, R. E., Precursory seismicity: Quiescence and clusters (abstract), Eos Trans. AGU, 60, 884, 1979.

Habermann, R. E., The quantitative recognition and evaluation of seismic quiescence: Appli-

cations to earthquake prediction and subduction zone tectonics, Ph.D. thesis, 253 pp., Univ. of Colo., Boulder, Colo., 1981.

Hagiwara, Y., Probability of earthquake occurrence as obtained from a Weibull distribution analysis of crustal strain, Tectonophysics, 23, 313-318, 1974.

Handshumacher, D. W., Post-Eocene plate tectonics of the eastern Pacific in The Geophysics of the Pacific Ocean Basin and Its Margin, Geophys. Monogr. Ser., vol 19, edited by G. D. Sutton et al., pp. 177-202, AGU, Washington, D. C., 1976.

Herron, E. M., Chile margin near 38°S: Evidence for a genetic relationship between continental and marine geological features or a case of curious coincidences?, in Nazca Plate: Crustal Deformation and Andean Convergence, edited by L. D. Kulm, J. Dymond, E. J. Dasch, and D. M. Hussong, Mem. Geol. Soc. Am., 154, 755-760, 1981.

Herron, E. M., S. C. Cande, and B. R. Ball, An active spreading center collides with a subduction zone: A geophysical survey of the Chile margin triple junction, in Nazca Plate: Crustal Deformation and Andean Convergence, edited by L. D. Kulm, J. Dymond, E. J. Dasch, and D. M. Hussong, Mem. Geol. Soc. Am, 154, 683-702, 1981.

Iida, K., D. C. Cox, and G. Pararas-Carayannis, Preliminary catalog of tsunamis occurring in the Pacific Ocean, Rep. HIG 67-10, 131 pp., Hawaii Inst. of Geophys., Univ. of Hawaii, Honolulu, 1967.

Jordan, T. E., B. L. Isacks, R. W. Allmendinger, J. A. Brewer, V. A. Ramos, and C. J Ando, Andean tectonics related to the geometry of the subducted Nazca plate, Geol. Soc. Am. Bull., 94, 341-361, 1983.

Kadinsky-Cade, K., and B. Isacks, Shallow structure of the Benioff zone in Chile (abstract), Eos Trans. AGU, 64, 264, 1983.

Kalbfleisch, J. D., and R. L. Prentice, Statistical Analysis of Failure Time Data, John Wiley, New York, 1980.

Kanamori, H., The energy release in great earthquakes, J. Geophys. Res., 82, 2981-2987, 1977a.

Kanamori, H., Seismic and aseismic slip along subduction zones and their tectonic implications, in Island Arcs, Deep Sea Trenches and Back-Arc Basins, Maurice Ewing Ser., vol. 1, edited by M. Talwani and W. C. Pitman III, pp. 163-174, AGU, Washington D. C., 1977b.

Kanamori, H., and D. L. Anderson, Theoretical basis of some emperical relations in seismology, Bull. Seismol. Soc. Am., 65, 1073-1095, 1975.

Kanamori, H., and K. McNally, Variable rupture mode of the subduction zone along the Ecuador-Colombia coast, Bull. Seismol. Soc. Am., 72, pp. 1241-1253, 1982.

Kapur, K. C., and L. R. Lamberson, Reliability in Engineering Design, 586 pp., John Wiley, New York, 1977.

Katz, H. R., Some new concepts on geosynclinal development and mountain building of the southern end of South America, Proc. Int. Geol. Congr., New Dehli, 22nd, 4, pp. 241-255, 1964.

Kelleher, J. A., Rupture zones of large South American earthquakes and some predictions, J. Geophys. Res., 77, 2087-2103, 1972.

Kelleher, J. A., L. R. Sykes, and J. Oliver, Possible criteria for predicting earthquake locations and their applications to major plate boundaries of the Pacific and Caribbean, J. Geophys. Res., 78, 2547- 2585, 1973.

Lawson, A., The California Earthquake of April 18, 1906, Report of the State Earthquake Investigation Commission, 2 vol. + atlas, Carnegie Institution of Washington, Washington, D. C., 1908.

Lehner, F. K., and V. C. Li, Large scale characteristics of plate boundary deformations related to postseismic readjustment of a thin asthenosphere, Rep. 23, 36 pp. Division of Engineering, Brown University, Providence, R. I., 1981.

Lomnitz, C., Statistical prediction of earthquakes, Rev. Geophys. Space Phys., 4, 377-393, 1966.

Lomnitz, C., Major earthquakes and tsunamis in Chile during the period 1535 to 1953, Geol. Rundsch., 59, 938-960, 1970.

Lomnitz, C., and F. A. Nava, The predictive value of seismic gaps, Bull. Seismol. Soc. Am., 73, 1815-1824, 1983.

Lowrie, A., and R. Hey, Geological and geophysical variations along the western margin of Chile near lat 33° to 36°S and their relation to Nazca plate subduction, in Nazca Plate: Crustal Deformation and Andean Convergence, edited by L. D. Kulm, J. Dymond, E. J. Dasch, and D. M. Hussong, Mem. Geol. Soc. Am, 154, 741-754, 1981.

Lyell, C., Principles of Geology, 9th ed., 835 pp., John Murray, London, 1853.

Malgrange, M. A. Deschamps, and R. Madariaga, Thrust and extension faulting under the Chilean coast: 1965, 1971 Aconcagua earthquakes, Geophys. J. R. Astron. Soc., 66, 313-331, 1981.

Mann, N. R., R. E. Schafer, and N. D. Singpurwalla, Methods for Statistical Analysis of Reliability and Life Data, 564 pp., John Wiley, New York, 1974.

McCann, W. R., S. P. Nishenko, L. R. Sykes, and J. Krause, Seismic gaps and plate tectonics: Seismic potential for major plate boundaries, in Proceedings of Conference VI, Methodology for Identifying Seismic Gaps and Soon-to-Break Gaps, U.S. Geol. Surv. Open File Rep., 78-943, 441-584, 1978.

McCann, W. R., S. P. Nishenko, L. R. Sykes, and J. Krause, Seismic gaps and plate tectonics: Seismic potential for major boundaries, Pure Appl. Geophys., 117, 1082-1147, 1979.

Mendoza, C., and J. W. Dewey, Seismicity associated with the great Colombia-Ecuador earthquakes of 1942, 1958 and 1979: Implications for barrier models of earthquake rupture, Bull. Seismol. Soc. Am., 74, 577-593, 1984.

Meyen, Dr., Letter in Foreign Quat. Rev, 13, 13, 1836.

Milne, J., The Peruvian earthquake of May 9th, 1877, Trans. Seismol. Soc. Jpn., 2, 50-96, 1880.

Minster, J. B., and T. H. Jordan, Present day plate motions, J. Geophys. Res., 83, 5331-5334, 1978.

Mogi, K., Some features of recent seismic

activity in and near Japan, Bull. Earthquake Res. Inst. Tokyo Univ., 46, 1225-1236, 1968.
Mogi, K., Relationship between the occurrence of great earthquakes and tectonic structures, Bull. Earthquake Res. Inst. Tokyo Univ., 47, 429-451, 1969.
Mogi, K., Seismicity in western Japan and long-term earthquake forecasting, in Earthquake Prediction: An International Review, Maurice Ewing Ser., vol. 4, edited by D. W. Simpson and P. G. Richards, pp. 43-52, AGU, Washington, D. C., 1981.
Nagume, T., Source regions of great earthquakes, Geophys. Mag., 35, 333-399, 1971.
Nishenko, S. P., Has the Valparaiso seismic gap started to rerupture? (abstract), Eos Trans. AGU, 63, 371, 1982.
Nishenko, S. P., and W. R. McCann, Seismic potential for the world's major plate boundaries: 1981, in Earthquake Prediction: An International Review, Maurice Ewing Ser., vol. 4, edited by D. W. Simpson and P. G. Richards, eds., pp. 20-28, AGU, Washington, D. C., 1981.
Ohtake, M. T., T. Matumoto, and G. V. Latham, Seismicity gap near Oaxaca, southern Mexico as a possible precursor to a large earthquake, Pure Appl. Geophys., 115, 375-385, 1977.
Pilger, R. H. Jr., Plate reconstructions, aseismic ridges and low-angle subduction beneath the Andes, Geol. Soc. Am. Bull., 92, 448-456, 1981.
Plafker, G., and J. C. Savage, Mechanism of the Chilean earthquakes of May 21 and 22, 1960, Geol. Soc. Am. Bull., 81, 1001-1030, 1970.
Prince, R. A., W. J. Schweller, W. T. Coulbourn, G. L. Shepard, G. E. Ness, and A. Masias, Bathymetry of the Peru-Chile continental margin and trench, 9 maps, scale 1:1,000,000, Map Chart Ser. MC-34, Geol. Soc. Am., Boulder, Colo., 1980.
Rikitake, T., Statistics of ultimate strain of the earth's crust and probability of earthquake recurrence, Tectonophysics, 26, 1-21, 1975.
Rikitake, T., Recurrence of great earthquakes at subduction zones, Tectonophysics, 35, 335-362, 1976a.
Rikitake, T., Earthquake Prediction, Dev. Solid Earth Geophys., vol. 9., 357 pp., Elsevier Scientific, New York, 1976b.
Robison, I., and Capt. Joy, Earthquake and rising of the sea coast of Chile in November 1822, Am. J. Sci., 30, 110-113, 1836.
Ruff, L., and H. Kanamori, Seismicity and the subduction process, Phys. Earth Planet. Inter., 23, 240-252, 1980.
Saint-Amand, P. (Ed.), Oceanographic, geologic and engineering studies of the Chilean earthquakes of May, 1960, Bull. Seismol. Soc. Am., 53, 1123-1414, 1963.
Saita, T., The great Chilean earthquake of January 24, 1939, Bull. Earthquake Res. Inst. Tokyo Univ., 18, 446-459, 1940.
Scholz, C., Scaling laws for large earthquakes: Consequences for physical models, Bull. Seismol. Soc. Am., 72, 1-14, 1982.
Schweller, W. J., L. D. Kulm, and R. A. Prince, Tectonics, structure and sedimentary framework of the Peru-Chile trench, in Nazca Plate: Deformation and Andean Convergence, edited by L. D. Kulm, J. Dymond, E. J. Dasch, and D. M. Hussong, Mem. Geol. Soc. Am., 154, 323-350, 1981.
Shimizaki, K., and T. Nakata, Time-predictable recurrence model for large earthquakes, Geophys. Res. Lett., 7, 279-282, 1980.
Sieh, K., Slip along the San Andreas fault associated with the great 1857 earthquake, Bull. Seismol. Soc. Am., 68, 1421-1448, 1978.
Silgado, E., History of the most noteworthy earthquakes in Peru (1513-1970), Geofis. Panam., 2, 179-243, 1973.
Steffen, H., Einige Ergebnisse der Untersuchungen Über das mittelchilenische Erdbeben vom 16 August 1906, Petermanns Mitt., 53, 132-138, 1907.
Sykes, L. R., Aftershock zones of great earthquakes, seismicity gaps and earthquake prediction for Alaska and the Aleutians, J. Geophys. Res., 76, 8021-8041, 1971.
Sykes, L. R. and S. P. Nishenko, Probabilities of occurrence of large plate rupturing earthquakes for the San Andreas, San Jacinto, and Imperial Faults, California, 1983-2003, J. Geophys. Res., 89, 5905-5928, 1984.
Sykes, L. R., and R. C. Quittmeyer, Repeat times of great earthquakes along simple plate boundaries, in Earthquake Prediction: An International Review, Maurice Ewing Ser., vol. 4, edited by D. W. Simpson and P. G. Richards, pp. 217-247, AGU, Washington, D. C., 1981.
Uyeda, S., and H. Kanamori, Back arc opening and the mode of subduction, J. Geophys. Res., 84, 1049-1061, 1979.
Ward, S. N., Earthquake mechanisms and tsunami generation: The Kurile Islands event of October 13, 1963 (abstract), Eos Trans. AGU, 62, 945, 1981.
Weibull, W., A statistical distribution function of wide application, J. Appl. Mech., 18, 293-297, 1951.
Winslow, M. A., The structural evolution of the Magallanes Basin and the neotectonics in the southernmost Andes, Antarctic Geosci., 4, 143-154, 1982.
Wortel, R., Age-dependent subduction of oceanic lithosphere, Ph.D. thesis, 147 pp., State Univ. of Utrecht, Utrecht, The Netherlands, 147 pp., 1980.
Wortel, M. J. .R., and N. J. Vlaar, Age dependent subduction of oceanic lithosphere beneath western South America, Phys. Earth Planet. Inter., 17, 201-208, 1978.

S. P. Nishenko, U. S. Geological Survey, P.O. Box 25046, MS 967, Denver Federal Center, Denver, CO 80225.

(Received February 17, 1983;
revised March 27, 1984;
accepted March 29, 1984.)

21